THE UNIVERSITY OF CALGARY

INTERACTIONS BETWEEN SELECTED SODIUM AND POTASSIUM CHANNEL BLOCKERS IN GUINEA PIG PAPILLARY MUSCLE

by

Li Wang

A THESIS

SUBMITTED TO THE FACULTY OF GRADUATE STUDIES

IN PARTIAL FULFILMENT OF THE REQUIREMENTS FOR THE

DEGREE OF MASTER OF SCIENCE

DEPARTMENT OF MEDICAL SCIENCE

CALGARY, ALBERTA

SEPTEMBER, 1991

ISBN 0-315-75253-X

THE UNIVERSITY OF CALGARY

FACULTY OF GRADUATE STUDIES

The undersigned certify that they have read, and recommend to the Faculty of Graduate Studies for acceptance, a thesis entitled, "Interactions Between Selected Sodium and Potassium Channel Blockers in Guinea Pig Papillary Muscle" submitted by Li Wang in partial fulfilment of the requirements for the degree of Master of Science.

Supervisor,
Doctor Henry J. Duff
Medicine

Doctor Wayne R. Giles
Medical Physiology

Doctor John V. Tyberg
Medicine and Medical Physiology

Doctor Jonathan C. Makielski
External Examiner
University of Chicago
Chicago, Illinois, U.S.A.

September 25, 1991

ABSTRACT

The interactions between prolongation of the action potential by a potassium channel blocker and reduction in the maximum upstroke velocity (V_{max}) of the cardiac action potential by sodium channel blockers were investigated in guinea pig papillary muscle using a conventional microelectrode technique. Agents which produce selective electrophysiologic effects were chosen. 1) Barium chloride (10^{-5}M) selectively blocks the inwardly rectifying potassium current, I_{K1}, and prolongs action potential duration. 2) O-demethyl-encainide (3×10^{-7}M) blocks activated sodium channels with slow kinetics of onset/offset of use-dependent block. 3) Mexiletine (4×10^{-6}M) blocks inactivated sodium channels with fast kinetics of onset/offset of use-dependent block.

To assess the interaction between partial blockade of I_{K1} and blockade of the inactivated sodium channels, we compared the effects produced by mexiletine alone to those by the combination of mexiletine and barium chloride. Mexiletine shortened action potential duration from 190 ± 14 msec (drug free) to 185 ± 13 msec ($p<0.05$). The addition of barium chloride to mexiletine significantly prolonged action potential duration from 185 ± 13 msec with mexiletine alone to 207 ± 15 msec ($p<0.05$). Mexiletine alone decreased V_{max} from 195 ± 29 V/s of drug free to 180 ± 26 V/s ($p<0.05$). While barium chloride had no effect on V_{max}, the addition of barium chloride to mexiletine further decreased V_{max} from 180 ± 26 V/s with mexiletine to 166 ± 18 V/s ($p<0.05$). To

assess the interaction between partial blockade of I_{K1} and blockade of the activated sodium channels, we compared the effects of O-demethyl-encainide and the combination of O-demethyl-encainide and barium chloride. O-demethyl-encainide slightly prolonged action potential duration from 174 ± 13 msec of drug free to 180 ± 15 msec. The combination of O-demethyl-encainide and barium chloride significantly prolonged action potential duration from 187 ± 15 msec with O-demethyl-encainide to 201 ± 15 msec with the combination of O-demethyl-encainide and barium chloride ($p < 0.01$). O-demethyl-encainide decreased V_{max} from 179 ± 17 V/s of drug free to 133 ± 15 V/s ($p < 0.01$). However, the addition of barium chloride to O-demethyl-encainide alone did not produce a further decrease in V_{max} as compared to O-demethy-encainide.

In summary, synergistic effect on V_{max} was observed when barium chloride, which prolongs the action potential and mexiletine which preferentially binds to the inactivated sodium channels were combined. In contrast, no synergistic effect on V_{max} occurred when barium chloride was added to O-demethyl-encainide which blocks the activated sodium channels. These results suggest that action potential prolongation may increase the proportion of the sodium channels in the inactivated state and thereby accentuate mexiletine interaction with the inactivated sodium channels. Prolongation of the action potential also decreased the diastolic interval during which mexiletine molecules can dissociate from the binding site resulting in an enhanced effect of mexiletine on V_{max}.

ACKNOWLEDGEMENTS

I wish to acknowledge the many contributions of the following individuals. Their considerable help will always be remembered.

First, I am profoundly grateful to Dr. Henry J. Duff who provided me with the opportunity to pursue my academic study. He has taught me the knowledge in cardiac electrophysiology and experimental techniques with great enthusiasm and patience. His tremendous help and thoughtfulness have been invaluable through out all my study. He has spent countless time reviewing my abstracts, papers, as well as this thesis. His guidance and support will always be appreciated.

My sincere gratitude to Dr. Wayne R. Giles, who was my interim supervisor during the time when Dr. Duff was on his sabbatical. He has provided me enormous help and guidance with his knowledge and expertise all through my study. He has given me invaluable teaching regarding fundamentals of cardiac electrophysiology and pharmacology. Furthermore, he has spent a great amount of time reviewing my abstracts, papers and thesis and has advised me about many of the ideas presented in this thesis.

A very special thank to Dr. John Tyberg who has always been very kind, enthusiastic and encouraging. He has been very friendly and

patient in answering all my questions, as well as reviewing my thesis and helping me to write better English.

A special acknowledgment also for Dr. Nipavan Chiamvimonvat whom I have collaborated on numerous studies. She has spent endless hours reviewing my thesis for format and content. She always answers my questions with unyielding patience. Her support and friendship combined with her talent make her considerable assistance immeasurable.

Special thanks to Dr. Robert Clark who took time to review my thesis and gave me many helpful suggestions. He has always given me very clear, precise and knowledgable answers to all my questions regarding this work.

Many thanks to Dr. Anne M. Gillis. She has given me suggestions and help for my thesis defence.

I would also like to acknowledge Margret Stemler and Tom thannhauser for their help with the instruments used in this study as well as Elaine Rude and Ela Thakore for the help with their technical expertise.

To my parents Luo Xiu Lian and Wang Yu Fu,

my husband Han Zhao Hua and my daughter Meng Meng

for their endless love and support from beginning to end.

For them, no words can express my deepest appreciation.

CONTENTS

LIST OF TABLES

LIST OF ILLUSTRATIONS

CHAPTER 1

BACKGROUND

1.1 Ionic Currents Underlying the Cardiac Action Potential

The configuration of the action potentials of cells from working myocardium (atrium and ventricle) can be described in five phases (Figure 1a) (1): Phase 0, the upstroke, or rapid depolarization; Phase 1, early rapid repolarization; Phase 2, the plateau; Phase 3, final repolarization; and Phase 4, the resting membrane potential. A diastolic depolarization is also observed during Phase 4 in pacemaking or specialized conducting tissue. The action potential results from ionic fluxes, and each ion moves primarily through its own selective channel(s) (2) as shown in Figure 1b. However, the configuration of the action potential has been found to be species-dependent and region-specific (3). Therefore the action potentials that generate any one heart beat vary shape, amplitude and duration as they propagate through electrically coupled cells within the whole heart. This pattern of events implies differences in underlying ionic currents during each action potential.

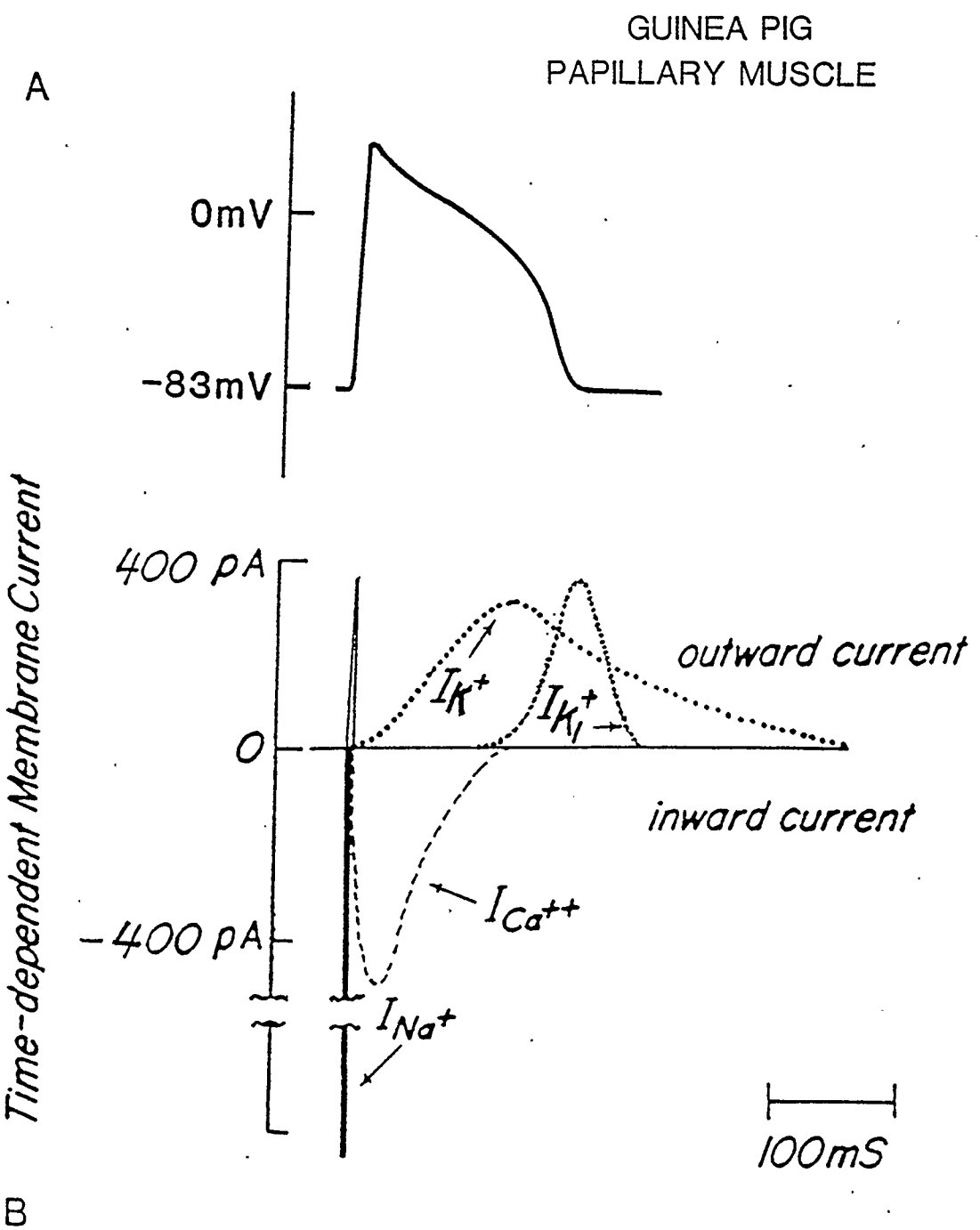
GUINEA PIG
PAPILLARY MUSCLE
A
0mV
-83mV
Time-dependent Membrane Current
400 pA
0
-400 pA
I_{K^+}
$I_{K_1^+}$
outward current
inward current
$I_{Ca^{++}}$
I_{Na^+}
100mS
B

Fig. 1-A, An action potential recorded from a guinea pig papillary muscle at 37°C. 1-B, Illustration of the time- and voltage-dependent ionic currents which underlie this action potential. Note the differences in (i) size, (ii) direction, (iii) ionic selectivity, and (iv) time course of these currents. I_{Na} shown as a "spike" to emphasize its speed and large size. The transient outward current(s) are not shown in this diagram (1-B was modified from Ref. 3).

A. Phase 0 - Transient Inward Sodium Current, I_{Na}

A large transient inward sodium current (I_{Na}) generates the initial rapid depolarization of the action potential (Phase 0) in most regions of the heart, with the exception of primary pacemaking tissue and some parts of atrio-ventricular node (4). The activation and inactivation of this current are time- and voltage-dependent (3). At the normal resting potential, most of the inactivation is removed and therefore the sodium channels are available to be activated (5). An electrical impulse propagating into resting tissue depolarizes the membrane sufficiently to activate the large and transient I_{Na} which drives the membrane potential toward the equilibrium potential for sodium (E_{Na}, approximately 50 mV). This transient sodium conductance lasts only a few milisecond, and then decays as the channels inactivate (Figure 2a) (6). The current-voltage relationship for I_{Na} shows a steep negative slope region between the voltages at - 60mV and -20 mV (Figure 2b), which is thought to be responsible for the all- or none feature of action potential propagation (6). Electrophysiological properties of the sodium channels will be discussed in detail in the later parts of this thesis.

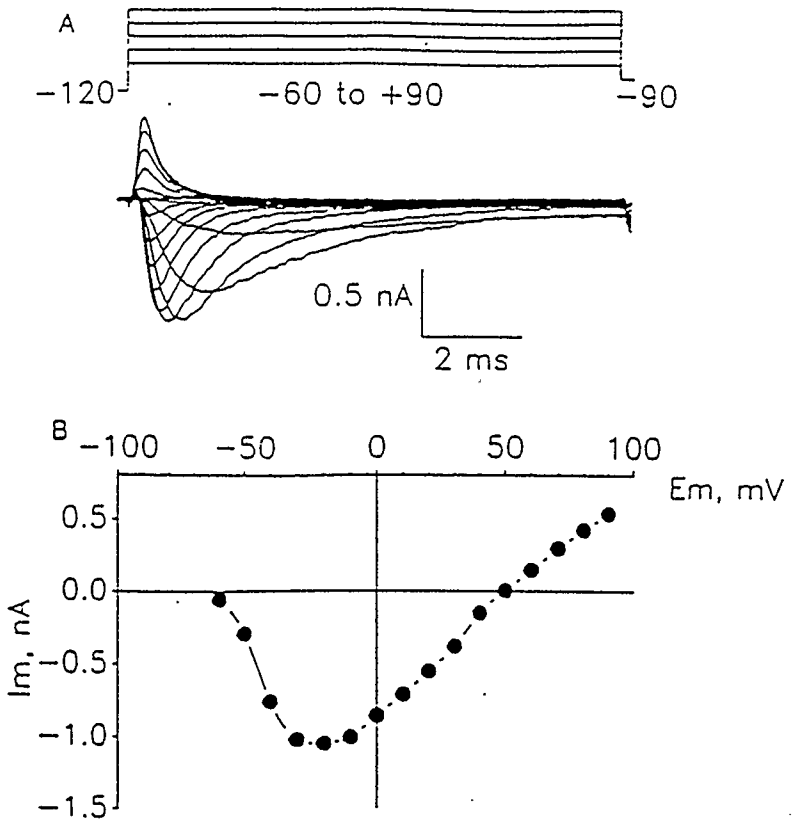

Fig. 2 Whole-cell Na^+-currents recorded from a neonatal rat ventricular myocyte. A, From a holding potential, -90 mV, a family of Na^+-currents (lower) was evoked by depolarizing test pulses. B, Peak Na^+-currents plotted against test pulse potential (peak current-voltage relationship). The external bathing solution was a modified Tyrode solution containing only 30 percent of normal [Na^+] to improve voltage control. The pipette solution contained 140 mM Cs^+ to block outward K^+ currents. The experiment was performed at room temperature (modified from Ref. 6).

B. Phase 1- Transient Outward Potassium Currents I_t and $I_{K(Ca)}$

Following Phase 0 of the action potential, the membrane repolarizes rapidly to near 0 mV, due to inactivation of I_{Na} as well as activation of outward currents carried by potassium ions. A transient outward potassium current (I_t) is activated at positive (plateau) potentials. This current can be partially inactivated at depolarized potentials, and recovers slowly after it has been inactivated, therefore, low frequency stimuli evoke a large transient outward current and prominent phase 1 of the action potential (7). I_t can be blocked by 4-aminopyridine (3) or quinidine (8). In heart, I_t has been reported in canine (9), sheep (10) and calf (11) Purkinje fibers and in rabbit (12), rat (13), canine (14) atrial and ventricular myocardium as well as in human atrium (8). However, I_t is thought to be largely absent in sheep, calf and guinea pig ventricle (9,15). Another potassium current which is partially responsible for Phase 1 is the calcium-activated potassium current, $I_{K(Ca)}$. This current is also time- and voltage-dependent. Its size and time course is modulated by intracellular calcium concentration and it can be blocked by inhibitors of the calcium current: cadmium and D-600; or inhibitors of calcium release from sarcoplasmic reticulum e. g. ryanodine (16). Repolarization due to these two outward potassium currents brings the membrane potential to near 0 mV, from which the plateau develops. In Purkinje fibers, Phase 1 is well defined and can be separated from Phase 2.

C. Phase 2-Transient Inward Calcium Current, I_{Ca}

During the plateau phase, a relatively small and slow inward calcium current is activated. It supplies the inward current which balances the outward current(s) and therefore maintains the membrane potential near 0 mV for more than 100 milliseconds in Purkinje fibers and working myocardial cells (17). In the atrium and ventricle, this net calcium entry also modulates the mechanical activity of the cell.

In Purkinje tissue, the sodium channels in the heart may also contribute to the plateau phase of the action potential as demonstrated by the observation that submaximal blocking concentrations of tetrodotoxin (TTX) reduce the plateau duration due to a decrease in the TTX-sensitive plateau sodium current (window current) with little changes in the maximum upstroke velocity (18-20). This window current was not found in the nerve and skeletal muscle.

D. Phase 3- Time- and Voltage-Dependent Outward Potassium Current, the Delayed Rectifier (I_K)

In Phase 3 of the action potential, repolarization proceeds rapidly due to inactivation of the slow inward calcium current and the activation of the time- and voltage-dependent potassium currents which drive the membrane potential back toward the equilibrium potential for potassium (E_K, approximately -98 mV) and fully repolarizes the cells. The type of the potassium current responsible for repolarization varies from region to region of the heart, as well as from species to species.

For example, in human atrium and rat ventricle, this potassium current is the large transient outward potassium current (I_t) (3). However, in guinea pig ventricle, the dominant repolarizing phase 3 current is the time- and voltage-dependent delayed rectifier potassium current, I_K. The kinetics of I_K are relatively slow and this current does not inactivate. Deactivation occurs when the membrane potential repolarizes to negative potential near the resting potential (3).

Once the membrane potential repolarizes to about -70 mV, the inwardly rectifying background potassium current, I_{K1}, is activated. The highly nonlinear current-voltage relationship of I_{K1} is shown in Figure 3. This I-V curve for I_{K1} illustrates that the magnitude of inward potassium current at membrane potential negative to E_K greatly exceeds the magnitude of outward current at positive potentials. Furthermore, when membrane potential is more positive than about -70 mV, the outward current becomes smaller and finally approaches zero at potentials of -10 mV (3,21).

The inward rectification of this potassium current has been inferred to play an important role in maintaining the plateau of the cardiac action potential since I_{K1} is very small at potentials corresponding to the plateau (22,23), and for generating a negative resting membrane potential in the ventricular myocardium (3), as well as in contributing an outward repolarizing current to the final phase of the action potential (21).

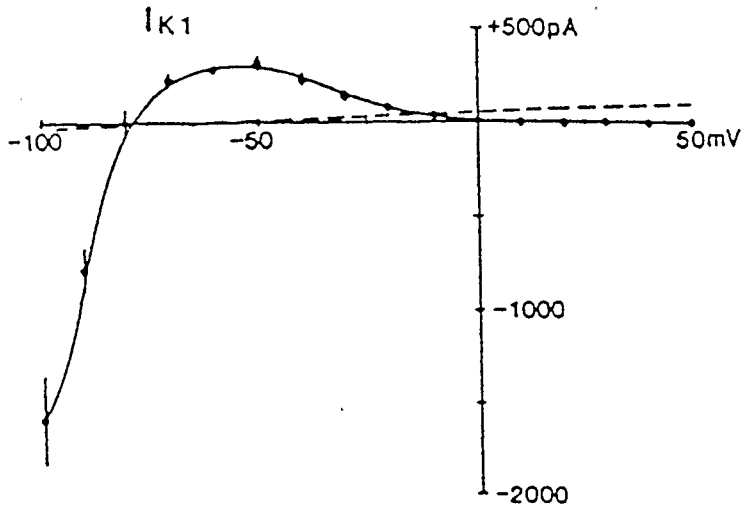

Fig. 3 A plot of current-voltage relationship for the inwardly rectifying K^+ current, I_{K1}, in the ventricle (modified from Ref. 3).

The mechanism of this rectification is now considered to be internal block by Mg^{2+}, possibly the result of rapid block of the open channel (21).

E. Phase 4- Resting Potential

Under normal conditions, the membrane potential of the working myocardium remains constant throughout diastole. The intracellular potential is 70 to 90 mV more negative relative to the outside of the cell, owing to the distribution of potassium ions across the cell membrane and resting potassium permeability. Potassium is the major ion determining the resting potential. The outward ionic current responsible for the resting membrane potential is the inwardly rectifying potassium current, I_{K1}. In addition, the Na-K pump current (I_p) in Purkinje tissue may also make a substantial contribution to maintaining the resting membrane potential.

1.2 Electrophysiology of the Sodium Current in heart

A sodium current is essential for the generation of the action potential in most excitable cells. As mentioned above, the initial upstroke of the cardiac action potential in many cardiac tissues, including ventricle, is due to a transient inward current caused by the influx of sodium ions through sodium channels. Based on the observation of the initial increase and subsequent decrease in sodium permeability during each action potential, Hodgkin and Huxley (24) first theorized that sodium channels cycle through three functionally distinct states during the action potential: the rested (R), the activated (A) and the inactivated (I) states. In the normal resting condition, for example, at a negative resting membrane potentials (-80

to -90mV), the sodium channels are predominantly in the rested state. There is therefore no sodium conductance, although most of the inactivation is removed and the channels are available to be activated. In the activated state, the sodium channels are open, and there is a time- and voltage-dependent sodium influx following depolarization. In the inactivated state, the sodium channels are closed at depolarized membrane potentials, and the sodium current decays rapidly (25). A transition from the inactivated to the rested state is considered to be a time- and voltage-dependent re-opening of the inactivation gate, and this process must occur before the channels are again available for activation. When applied to cardiac tissue, these different sodium-channel states mean that the rested state is most prevalent during diastole, the activated state during the upstroke of the action potential, and the inactivated state during the plateau of the action potential or when the tissue is artificially depolarized (e.g., by ischemia) (25)

Hodgkin and Huxley provided a mathematical model (H-H model) to describe the kinetics of the observed macroscopic sodium currents recorded using the voltage-clamp technique in squid axon (24). They observed that activation of the sodium channel is steeply voltage-dependent followed by inactivation. The activation process exhibits a small delay, which implies that the channel must have several underlying steps controlling the opening event. Therefore, they proposed that this steep voltage-dependent activation may involve transmembrane movements of the charges (gating charge particles or gates) and that

this charge movement could produce a small electrical current (gating current). As expressed in H-H model, these steps are represented by m and h gates with three m gates controlling activation and one h gate controlling inactivation (24). The probability that all gates are in open position is $m^3 h$, and therefore I_{Na} can be represented by $m^3 h \bar{g}_{Na} (E-E_{Na})$ where $\bar{g}_{Na}$ represents the maximum conductance of the sodium channel, E represents the membrane potential and E_{Na} represents the equilibrium potential for sodium ions. According to this model, the opening and closing reactions of the conductance gates are independent, both of which respond directly to membrane potential. Activation gates (m gates) open rapidly and inactivation gate (h gate) closes relatively slowly (24).

The gating current predicted by Hodgkin-Huxley was detected by Armstrong et al (26-28). However, analysis of the "on" and the "off" gating current suggests that activation gating and inactivation gating are kinetically coupled in some way, which contrasts with the independent "m" and "h" processes in Hodgkin-Huxley equation. Recently, single channel recordings show that upon depolarization from a negative level to one above threshold, the channel opens after a variable delay. Some channels open after a long delay, after the ensemble current has begun to decline. The delay of the whole cell current is a consequence of fewer channels openning during that time, rather than the Hodgkin-Huxley explanation of channel inactivation (29). In addition, it has been shown that inactivation of sodium current is more complex than that described in the H-H model both in nerve and heart (6, 30-32).

Kunze et al (31) and Brown et al (6, 32) found that cardiac sodium channel inactivation consists of at least two rate constants (fast and slow). The slow components may contribute to the plateau of the cardiac action potential. Even though these discrepancies from the H-H model have become apparent, this model is, nevertheless, still a framework for the study of sodium channel kinetics. The two current models for the mechanisms of class I antiarrhythmic drugs, the modulated and the guarded receptor models, are based on the concepts of the channel states and channel gates, respectively.

Recently, the primary structures of the sodium channels from rat brain have been elucidated by cloning and sequencing the complementary DNAs (33-35). The sodium channel is composed of about 2000 amino-acid residues and contains four homologous trans-membrane repeats (I-IV), each of which has six membrane-spanning segments (S1-S6) (Figure 4). The positive charged amino acids at each third position in segment 4 (S4) of repeat I constitute at least part of the gating charge involved in the voltage-dependent activation of the sodium channel (29,36), and it is the best candidate for the channel's voltage sensor. The linkage between repeats III and IV of the sodium channels located on the cytoplasmic side of the membrane is implicated by mutation and antibody studies to be involved in inactivation of the sodium channel (29,36).

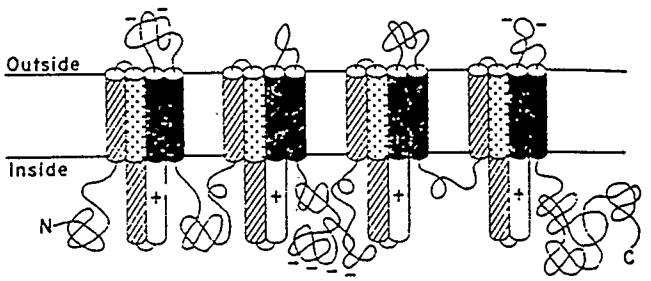

Fig. 4 Proposed transmembrane topology of a sodium channel. The four homologous domains spanning the membrane are displayed schematically. Segments S1-S6 in each repeat (I-IV) are indicated by cylinders as follows: S1, cross-hatched; S2, stippled; S3, hatched; S4, indicated by a plus sign; S5 and S6, solid (modified from Ref. 34).

1.3 Class I Antiarrhythmic Drugs and Their Subclassification

Class I antiarrhythmic drugs are often used in the treatment of cardiac arrhythmias. The main action of this class of antiarrhythmic drugs is blockade of the sodium channels resulting in depression of the maximum upstroke velocity (V_{max}) of the cardiac action potentials (37). Class I antiarrhythmic drugs have been subclassified into three groups (Ia,Ib and Ic) based on differences in their kinetics of interaction with the sodium channels and their differential effects on action potential duration (38,39). Class Ib drugs, such as mexiletine, block the sodium channel with fast rate constants of binding/unbinding and shorten action potential duration. Class Ic drugs, such as encainide, have very slow rate constants of binding/unbinding with only slight effect on action potential duration. Class Ia drugs, such as quinidine, block the sodium channel with intermediate association and dissociation rate constants and cause a prolongation of action potential duration. There are known limitations to this classification scheme. The most important limitation is that the currently available antiarrhythmic drugs have multiple actions. For example, The effects of the action potential prolongation and decrease in V_{max} produced by quinidine seem to be a combination of class I and class III properties. In addition, the metabolites of the drugs often have actions different from their "parent" compound (39,40).

1.4 Use-Dependent Block of Sodium Channels

Use-dependent block refers to the accumulated increase in the degree of channel blockade with repetitive depolarization. Unless a sodium channel blocker has exactly the same affinity for rested, activated and inactivated channel states, and the voltage- and time-dependence of gating does not change when the drug is bound to the channel, its action on the sodium current will be use-dependent under appropriate conditions (41). Use-dependent block has two major features: frequency-dependence and voltage-dependence. It has been observed that the degree of blockade of the sodium channel by a wide variety of local anesthetics and class I antiarrhythmic drugs depends on stimulation rate. High-frequency stimulation usually causes more blockade than low-frequency stimulation (42-44), since the rest interval is too short for the channel to be completely freed of the blocker. Therefore with higher stimulation frequency, fewer drug molecules will dissociate from binding sites and the more blockade will result. Secondly, it has been observed that class I antiarrhythmic agents are more effective in depolarized tissue than in tissue with a normal resting membrane potential (45). Since most antiarrhythmic agents are assumed to have a very low affinity for the rested state but high affinity for either activated or inactivated states, an increase in the degree of channel blockade is expected in depolarized tissue where more channels are in the inactivated state. Another aspect of the voltage-dependent block is that channel gating behavior is voltage sensitive,

as a result, access of certain drugs to the receptor may be voltage-dependent. Use-dependent block is thought to be the characteristic feature of class I antiarrhythmic drugs. Therefore, a framework that explains use-dependent block may be important in understanding the mechanisms of action of Class I antiarrhythmic agents.

1.5 Models for Mechanisms of Action of Sodium Channel Blockers

A. Modulated Receptor Hypothesis

To explain use-dependent block of class I antiarrhythmic drugs, Hille (46) and Hondeghem and Katzung (45) used channel state theory based on the HH model and proposed the modulated receptor hypothesis, in which antiarrhythmic drugs bind preferentially to certain channel states (Figure 5) (47). Binding occurs with state-specific association and dissociation rate constants. This model also postulates that (i) drug-associated channels do not conduct, even in the activated state, and (ii) drug-associated channels have altered kinetics of recovery from the inactivated state. According to the modulated receptor hypothesis, the ability of a drug to bind to a particular state of the channel depends upon the duration of the state and the state-specific rate constants.

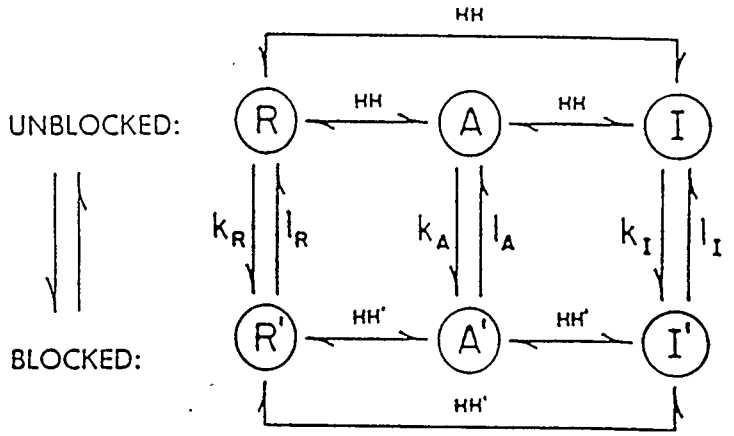

Fig. 5 Diagram of the modulated receptor mechanism for antiarrhythmic drug action. R = rested; A = activated; I = inactivated drug-free fractions of the population of sodium channels; R′, A′ and I′= the respective states for the drug-associated fractions; HH = standard Hodgkin-Huxley rate constant; HH′ = the same rate constant but voltage-dependence altered by drug binding; K_R, K_A and K_I represent the association rate constants, while I_R, I_A and I_I represent the dissociation rate constant for the respective channel fractions (modified from Ref. 47).

For a blocker with fast time constants of both onset and recovery from block, block develops and then dissipates rapidly during each action potential. Therefore, there is little augmentation of block by subsequent depolarizations. However, for many agents (e.g., quinidine), the rate of drug dissociation is slow enough that there is still residual sodium channel blockade between beats at physiologic heart rates. Consequently, quinidine can effectively depress conduction of impulses arising at any time during diastole. In contrast, lidocaine binds preferentially to inactivated channels with fast kinetics. The latter therefore results in use-dependent block only at fast stimulation rates or with application of early extrastimuli, which theoretically allow accumulation of the inactivation state of the sodium channels leading to enhanced interaction of lidocaine with the inactivation state. On this basis, Hondeghem and Katzung (47,48) hypothesized that additional depression in conduction of early diastolic impulses could be obtained by combining selected class I "slow" agent with a "fast" agent, in particular, if the two agents also interact preferentially with different channel states as mentioned above. This prediction has been supported by the results from canine models of rhythm disturbances as well as from patients with ventricular arrhythmias (49-51).

B. Guarded Receptor Hypothesis

The guarded receptor hypothesis was proposed by Starmer et al (52). It shares several features with the modulated receptor hypothesis. Both models are based on Hodgkin-Huxley theory. In addition, both models postulate that drug-associated channels cannot conduct. However, the guarded receptor hypothesis assumes that the affinity of a drug for the receptor is constant. In this hypothesis, the channel gates restrict drug access to and egress from its binding site. Therefore, the channel gates control the binding of drug to its receptor. On binding drug to a receptor, the movement of the channel gates is limited, which may lead to block the sodium influx (50). The guarded receptor hypothesis is a useful framework for understanding the blockade of sodium channels produced by a positively charged drug which can not penetrate membrane. The drug can bind to the channel receptor only when the channel is open.

Both the modulated receptor hypothesis and the guarded receptor hypothesis predict the presence of a receptor for Class I antiarrhythmic drugs. Using biochemical technique, Sheldon and Duff et al have shown evidence for the presence of a receptor for class I antiarrhythmic drugs associated with cardiac sodium channels (53). They have shown that the binding of antiarrhythmic drugs to this site is saturable, reversible and occurs at pharmacologically relevant concentrations with similar rank order of potency in vivo and in vitro. Stereospecificity is a further feature of characteristic of receptor

binding. It has been reported in an isolated perfused heart preparation that the R(-) isomer of tocainide was significantly more effective than its S(+) isomer in prolonging conduction time (54). This effect was associated with the higher affinity of the R(-) than the S(+) in the binding sites. Stereospecificity has also been demonstrated in several other pairs of antiarrhythmic drugs. For example, quinidine, a R(-) isomer, is more effective than its S(+) isomer, quinine. Furthermore, it has been reported that perhaps cardiac sodium channels have an additional external binding site (55). Therefore, at least some of the properties of antiarrhythmic interaction with the cardiac sodium channels may be the results of kinetic effects mediated by binding to this external site.

1.6 Combinations of Antiarrhythmic Drugs

Recently, clinical reports of the effectiveness of antiarrhythmic therapy have shown that the combination of class Ia and Ib agents with varied electrophysiologic properties often results in a more effective antiarrhythmic actions with fewer side effects than does the administration of either single agent, so called "mono-therapy" (49, 56-58). Duff et al first studied the combination of quinidine and mexiletine in patients with premature ventricular complexes (PVC) who were evaluated by 24-hour Holter recordings (49). They found this combination therapy to be more effective in suppression of premature ventricular complexes (86 ± 26%) than quinidine (59 ± 16%) or mexiletine alone (63 ± 25%). Greenspan et al (56) also reported that

the combination of quinidine and mexiletine therapy produced enhanced antiarrhythmic efficacy as compared to either drug alone in 23 patients with inducible sustained ventricular tachyarrhythmias (VT). This combination prevented induction of ventricular tachyarrhythmias in 8 of 23 patients vs 0 of 23 patients with single drug, and in 15 patients, this combination therapy significantly prolonged the tachycardia cycle length and reduced the symptoms associated with the induced arrhythmia. More recently, Giardina and Wechsler (58) have reported that results in patients with frequent premature ventricular complexes and nonsustained ventricular tachyarrhythmias, even lower doses of quinidine and mexiletine than those used in the previous studies suppressed 80% of premature ventricular complexes in 13 of 14 patients and suppressed 100% of episodes of ventricular tachyarrhythmias in 6 of 8 patients. Monotherapy was less effective; 80% suppression of premature ventricular complex was observed in only 5 of 15 patients and 100% suppression of ventricular tachyarrhythmias in 2 of 9 patients. Moreover, this combination therapy was better tolerated than are standard doses of quinidine. Thus, combination of quinidine and mexiletine has been shown to be an effective therapy for sustained ventricular tachycardia, even in patients refractory to mono-therapy.

The antiarrhythmic and electrophysiologic effects of the combination of class Ia and Class Ib agents have also been evaluated in both isolated perfused heart and intact animal models (59-63). However, there are some discrepancies amongst these reports. In ischemic models (60,61) where ventricular tachycardias were induced by programmed

electrical stimulation, combination of quinidine and mexiletine produced an enhanced antiarrhythmic activity associated with prolongation of both conduction time and refractoriness in the infarct zone. However, this pattern of results is different from that obtained by Costand et al in the open chest noninfarcted canine preparation (62,63), in which the same drug combination produced a greater post-repolarization refractoriness but less slowing of the conduction time than mono-therapy. The differences in the effects of combination therapy upon the conduction time in these two studies may result from the two different preparations used.

Other discrepancies exist among in vitro studies of various combinations of class Ia and Ib agents. Valois et al (64) studied the interaction between quinidine and tocainide (class Ib drug) in dog Purkinje fibers. They found that the extent of use-dependent block of V_{max} seen with the combination of quinidine and tocainide was approximately equivalent to that seen with quinidine alone. However, at more rapid pacing rates the extent of total block was increased. In contrast to the results of Valois, Valenzuela et al (65) reported that in guinea pig papillary muscle the combination of quinidine and mexiletine produced a greater tonic block and a less use-dependent block of V_{max} compared to those seen with quinidine alone. Furthermore, quinidine prolonged action potential duration in Purkinje fibers from Valois' study whereas quinidine shortened action potential duration in ventricular muscle in Valenzuela's study. Although these discrepancies may result from different tissue used, it is unknown

whether changes in action potential duration can make any contributions to the enhanced antiarrhythmic efficacy produced by the drug combinations.

Recently, some data suggest that prolongation of action potential duration may play an important role in the enhanced antiarrhythmic efficacy produced by the combination of quinidine and mexiletine (66, 67). Duff et al reported that combination of a low concentration of tetrodotoxin (a selective sodium channel blocker) and quinidine (a sodium channel blocker which also prolongs action potential duration) produced the antiarrhythmic activity similar to those seen with combination of mexiletine and quinidine (66). In contrast, the combination of mexiletine and tetrodotoxin did not produce enhanced antiarrhythmic or synergistic electrophysiologic effects. This lack of enhanced antiarrhythmic activity may be due to the fact that the combination of mexiletine and tetrodotoxin did not include an agent which prolongs action potential duration. Duff et al (67) also compared antiarrhythmic effects when mexiletine was combined with either quinidine or quinine (a stereoisomer of quinidine). Quinidine and quinine produced equivalent sodium channel blockade but only quinidine prolonged action potential duration. The antiarrhythmic activity of combination of mexiletine and quinidine was significantly greater than that of combination of mexiletine and quinine. These data obtained suggest that prolongation of action potential duration may play an important role in the enhanced antiarrhythmic activity produced by combination of mexiletine and quinidine. Although, the ionic

mechanisms are not known, these findings provided the rationale for the present investigation, that is whether prolongation of the action potential may modulate the effects of sodium channel blockers.

CHAPTER 2

HYPOTHESES

We have hypothesized the following three mechanisms for the enhanced electrophysiologic effects seen with the combination of quinidine (class Ia) and mexiletine (class Ib).

Hypothesis I: Enhanced electrophysiologic effects occur when a drug which causes use-dependent sodium channel block(UDB) with slow onset/offset kinetics is combined with a drug which causes use-dependent block with fast onset/offset kinetics.

Hypothesis II: Enhanced electrophysiologic effects occur when a drug which prolongs action potential duration by blocking the repolarizing potassium currents is combined with a drug which binds preferentially to inactivated sodium channels.

Hypothesis III: Enhanced electrophysiologic effects occur when all three properties (sodium-channel blockade with slow kinetics, sodium channel blockade with fast kinetics, and prolongation of action potential duration produced by potassium channel blockade) are combined. All three hypotheses are illustrated in the figure 6.

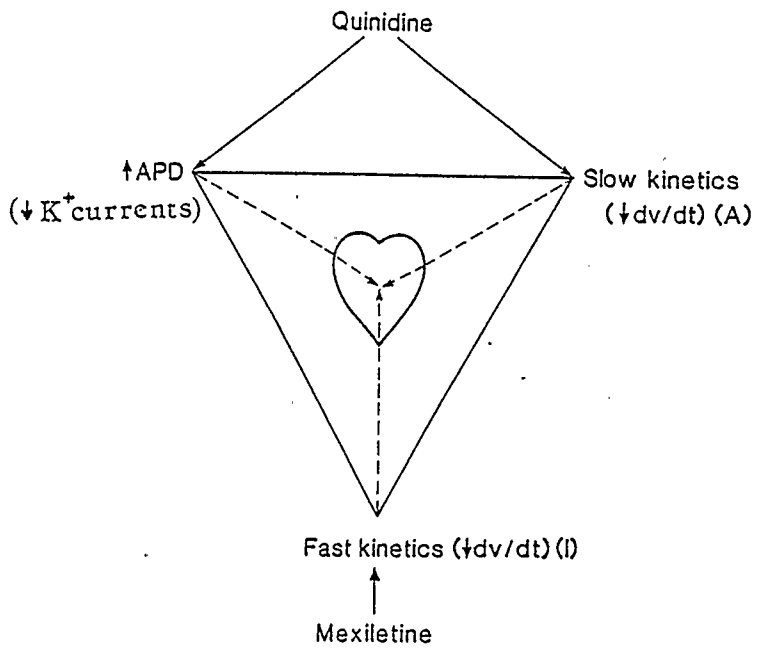

Fig. 6 Diagram of our hypotheses for the mechanism(s) of the combined electrophysiologic effects of Class Ia and Class Ib antiarrhythmic agents. For details of the hypotheses see text.

CHAPTER 3

METHODS

3.1 Rationale for Selection of the Drugs Used in This Study

Since quinidine produces multiple electrophysiologic effects, it is not possible to use quinidine to prolong action potential duration selectively or to decrease V_{max} selectively. In order to test our three hypotheses, the following two agents which produce selective electrophysiologic effects were chosen as the model drugs (to mimic the actions of quinidine). Barium chloride at low concentration (Ba, 10^{-5}M) selectively blocks I_{K1} and prolongs action potential duration without any effect on other repolarizing potassium currents or depolarizing inward currents (68,69). The second model drug is O-demethyl encainide (ODME, 3×10^{-7}M), a metabolite of encainide, which selectively blocks the activated state of the sodium channels with slow kinetics of onset and recovery from use-dependent block similar to quinidine (70). These two "model" drugs were used alone or in combination with mexiletine (Mex, 4×10^{-6}M) which preferentially blocks the inactivated state of the sodium channels with fast kinetics of onset and recovery from use-dependent block (37,71).

3.2 Rationale for Choosing Guinea Pig Papillary Muscle for these Experiments

The reasons that guinea pig papillary muscles were chosen for this study are as follows. The characteristics of the cardiac sodium current are similar in different mammalian tissue. In contrast, the potassium currents are species dependent as well as region specific (68). For example, the inwardly rectifying background potassium current (I_{k1}) is much larger in guinea pig ventricles than it is in the atria (71) and this is the principal current responsible for final repolarization of the action potential. Since block of I_{k1} by barium chloride is selective, it is possible to use barium chloride in combination with different sodium channel blockers to study the effects of action potential prolongation on the degree of sodium channel blockade. Guinea pig papillary muscles are relatively small and can be superfused adequately. Finally, previous experiments on the drug combination *in vitro* have been done mainly in guinea pig papillary muscles. Guinea pig papillary muscles were therefore used in our experiments, so that data can be compared with those of previous studies, such as Valenzuela's study (65).

3.3 Preparation and Recording Solution

Guinea pigs of either sex, weighing 250-300 grams were anesthetized with sodium pentobarbital (40 mg/kg); this was followed by cervical dislocation. Their hearts were excised rapidly and placed in

oxygenated HEPES buffered solution for subsequent dissection. The solution contained (in mM): sodium chloride 128, potassium chloride 5, calcium chloride 1.1, magnesium chloride 1, sodium-acetate 2.8, dextrose 10, HEPES 10 and sodium hydroxide 10 (pH 7.4 ± 0.01). Papillary muscles of 4-7 mm in length and 1 mm or less in diameter were excised from right ventricle. The tendinous end of the muscle was pinned to the bottom of a Sylgard coated lucite muscle chamber. The tissue was superfused with HEPES buffered solution at a rate of 8 ml per minute at 37 ± 0.3°C, which was measured by a thermocouple probe close to the tissue (within 2 mm). Bipolar electrodes insulated with teflon except at the tips were used to stimulate tissue using a programmable stimulator (Bloom Associates), with constant current pulse of 2 msec in duration at twice the diastolic threshold current. Each preparation was equilibrated in the bath for at least two hours before a microeletrode impalement was made.

3.4 Electrophysiologic Studies

Electrophysiologic studies were performed using conventional microelectrode techniques. The intracellular micropipette was prepared by pulling a heated glass capillary tube to a sharp point (approximate 0.5 μM) that still has an opening at the tip. The micropipette was then filled with a conducting solution (3 M KCl) having a tip resistance of 10-20 Megohms and used to record transmembrane potentials. The shank of the pipette was coupled to an Ag-AgCl half-cell which was then connected to a high impedance amplifier (Figure 7) (A-M systems,

Inc., WA, USA). The ground lead of the amplifier was attached via another Ag-AgCl electrode to the bath solution. To measure the changes in the membrane potential, the glass microelectrode was first dipped into the bath and the amplifier was zeroed. The microelectrode was then slowly and carefully advanced into a cell at which point a negative transmembrane potential was recorded. The transmembrane potentials, which were more negative than -78mV were accepted in this study.

Transmembrane potential signals were displayed on a storage oscilloscope (Hitachi, 10 MHz) and were converted into digital form using a Techmar 100 KHz A/D converter with a conversion interval of 25 msec. The first derivative of the transmembrane potential was obtained using an electronic differentiator which is linear between 10 and 1,000 volts per second (dv/dt). The differentiated signal was displayed on the oscilloscope and passed through a sample-and-hold circuit. An IBM AT computer with a custom made software routine (BASCOM Consultants, Montreal, Canada) was used to measure the resting membrane potential; action potential duration at 50%, 90% and 95% repolarization; total amplitude and amplitude of the overshoot of the action potential; and V_{max}.

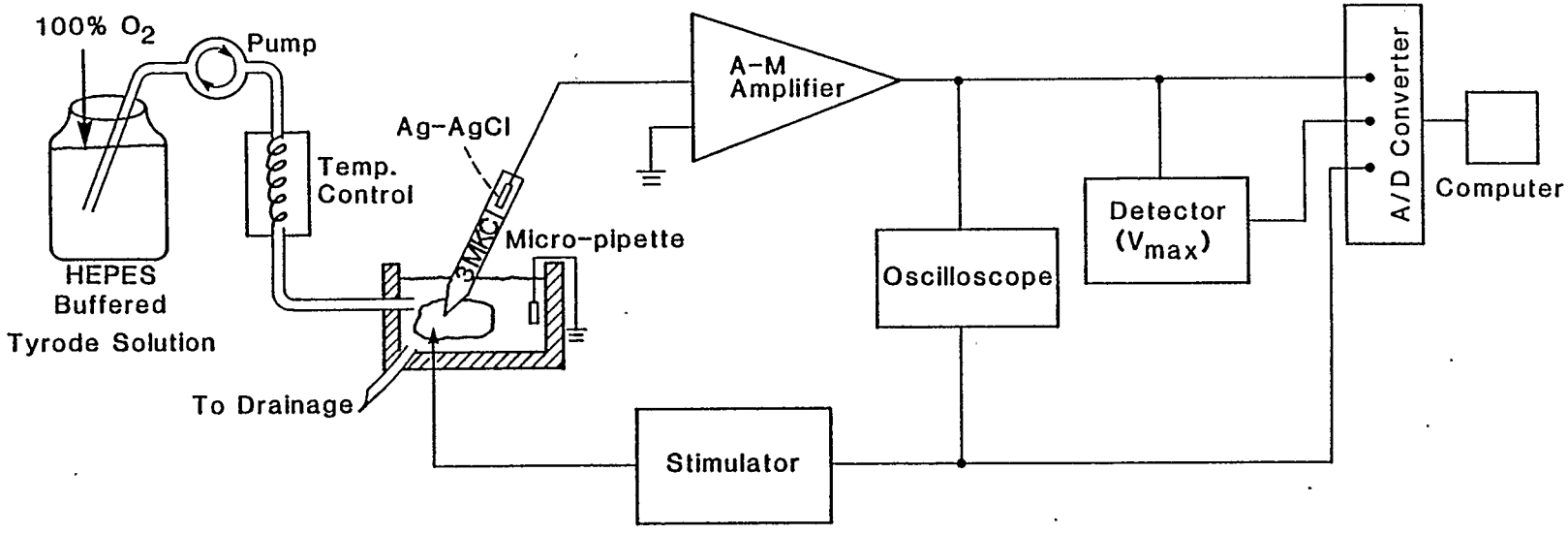

Fig. 7 Illustration of the instruments used for measurement of the membrane potential in this study

The instruments used in this study were calibrated. Square waves with known voltages, amplitudes and pulse widths were used as control inputs. The signals were delivered through the probe tip of the microelectrode holder and different parameters including voltage, amplitude and pulse width of the signals were recorded through the computer. The noise calibration was also recorded by superimposing 60 Hz noise (with different noise amplitudes) upon the signal. Similarly, measurement of V_{max} with this system was tested by using triangular waves (the slope of triangular wave was the desired V_{max}). Then, the test results from computer were plotted as functions of the known control input values (reading from Nicolet oscilloscope) and linear regression was used to obtain R-values, slopes and Y-intercepts. The calibration results are shown in figure 8.

Calibration

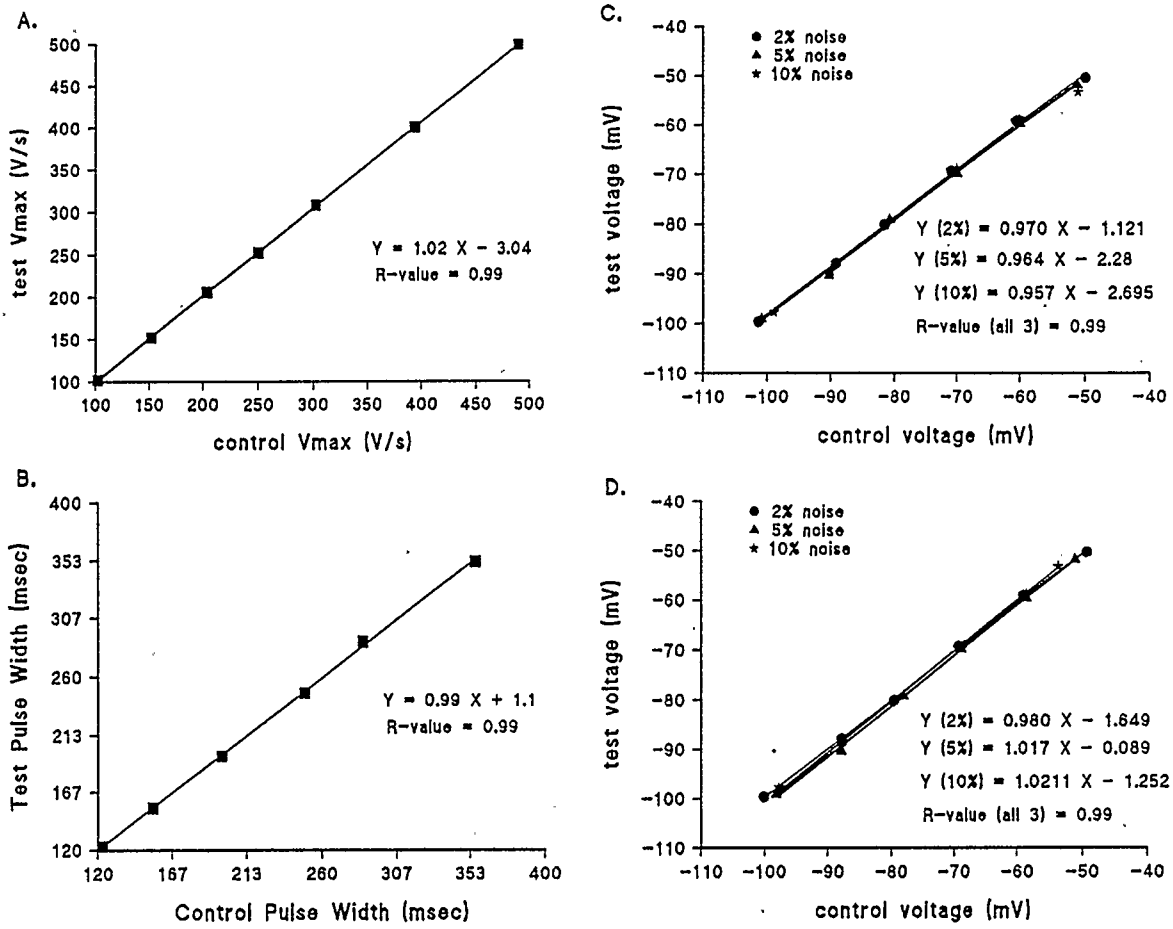

Fig. 8 Results of calibration procedures. A, Calibration for V_{max}. B, Calibration for pulse width (duration). C, Calibration with 60 Hz noise for voltage. D, Calibration with 60 Hz noise vs no 60 Hz noise.

3.5 Protocols Used for the Assessment of Refractoriness, Kinetics of Use-Dependent Block and Recovery as well as Tonic Block

After steady-state pacing at a basic cycle length of 500 msec, the ventricular effective refractory period was measured by applying an extrastimulus (S_2) at progressively shorter coupling intervals until an action potential could no longer elicited. A 3-sec rest period was given between each stimulus train. Onset of use-dependent block and recovery from use-dependent block was assessed after steady state pacing, which was defined as continuous pacing at a cycle length of 500 msec for at least 2 minutes. To measure the development of use-dependent decrease in V_{max}, the preparations were stimulated after a 2-min rest period with a 100-beat train at a cycle length of 500 msec. The V_{max} of each action potential in the train after the rest period was measured. To assess the kinetics of recovery from use-dependent block, the preparation was paced at a constant cycle of 500 msec until the use-dependent block reached the steady state. The pacing train was then followed by a variable rest period (S_1, S_2 coupling interval). The rest period was measured as the diastolic interval which was defined as the interval between the time at which the cell had repolarized to within 1 mV of its maximum diastolic potential and the next stimulus artifact. Tonic block is the drug-induced sodium channel block persisting after a long rest period (25). Tonic block does not only represent block of the rested channels but also can result from block of the open channels that develop at any time before the maximum activation of the sodium channel. Tonic block was determined

by calculating the ratio of V_{max} for the first pulse after a long rest period in drugs to the V_{max} at drug free.

3.6 Drug Combination Sequences

After the electrophysiologic parameters were evaluated under control conditions, the same stimulation protocols were repeated 30 min after each drug treatment. The drug treatments were given in the following randomized sequences (Figure 9): 1) control followed by O-demethyl-encainide (3×10^{-7}M) alo ne, followed by O-demethyl-encainide (3×10^{-7}M) and mexiletine (4×10^{-6}M) in combination, followed by O-demethyl-encainide, mexiletine and barium chloride (1×10^{-5}M) in combination; 2) control followed by O-demethyl-encainide alone, followed by O-demethyl-encainide and barium chloride in combination followed by O-demethyl-encainide, barium chloride and mexiletine in combination. 3) control followed by mexiletine alone followed by mexiletine and barium chloride in combination; 4) control followed by barium chloride alone followed by washout; 5) control followed by placebo treatment followed by a second placebo treatment. The concentrations of O-demethyl-encainide and mexiletine were selected according to therapeutic concentrations in clinical setting. In order to evaluate recovery from use-dependent block a concentration of 1.5×10^{-6}M of O-demethyl-encainide was used. Only experiments in which the impalement was maintained in a single cell throughout the experiments were included.

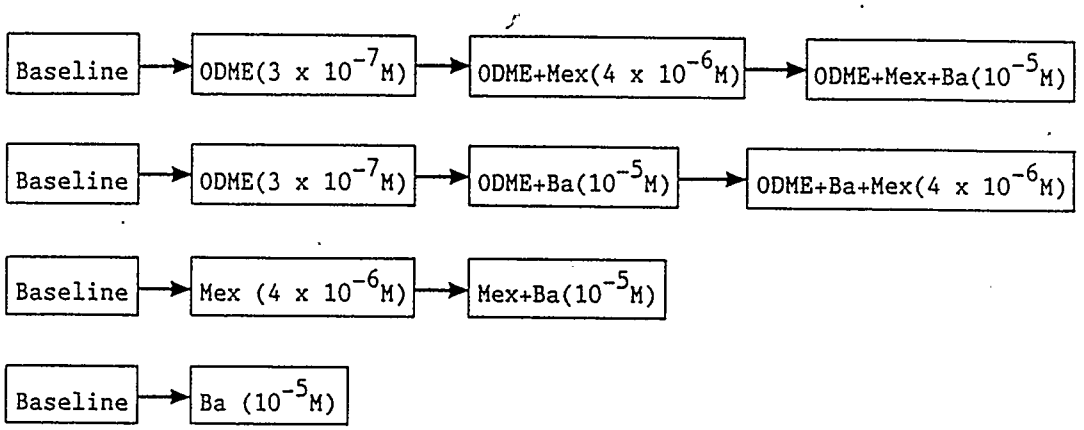

Fig. 9 A diagram of the drug combination sequences used in this study.

3.7 Statistics

Data are expressed as mean ± standard deviation(SD). Analysis of variance (ANOVA) was used to examine the differences among the multiple groups. The student's t-test was used to determine the differences between paired observations. For data which were compared more than once, the Bonferoni correction was used. A nonlinear least-squares fitting routine was used to determine the rate constants for the onset of use-dependent block and the recovery from use-dependent block. All the data were first fit to a single exponential equation to derive a time constant (τ) of use-dependent block and recovery from use-dependent block. If the experimental data could not be fitted by the single exponential equation, then a biexponential equation was used to obtain time constants (τ_f and τ_s). The null hypothesis was rejected when the two-tailed p value was less than 0.05.

In this study, the enhanced electrophysiologic activity was refered to a greater prolongation of action potential duration and refractoriness as well as a greater decrease in V_{max} as compared to a single drug treatment. The synergistic effect in this study means that the total effect was significantly more than additive effect produced by the drug combination.

CHAPTER 4

RESULTS

4.1 Drug-Induced Effects on Refractoriness, Action Potential Duration and Steady State V_{max}

The electrophysiologic effects of O-demethyl-encainide (3×10^{-7}M), mexiletine (4×10^{-6} M), barium chloride (10^{-5} M), and their combinations were studied in guinea pig papillary muscles driven at basic cycle lengths of 500 msec (2 Hz). Resting membrane potential, action potential duration and V_{max} were not significantly altered after a 2-hour placebo treatment (Table 1). As shown in Tables 2 and 3, none of drug treatments significantly affected resting membrane potential. The changes in refractoriness generally paralleled the changes in action potential duration with different drug treatments. For example, mexiletine shortened action potential duration slightly (-5 ± 3 msec) compared to baseline ($p< 0.05$), and also slightly shortened refractoriness (-3 ± 6 msec). O-demethyl-encainide slightly prolonged action potential duration (6 ± 5 msec) ($p< 0.05$) and produced a small increase in refractoriness (9 ± 3 msec) ($p< 0.05$). Barium chloride increased action potential duration by 20 ± 4 msec (Figure 10) and increased refractoriness by 17 ± 3 msec. Similarly, the combination of O-demethyl-encainide and barium chloride produced a substantial prolongation in refractoriness (30 ± 6 msec), which was associated with a significant prolongation of the action potential duration (23 ± 2 msec) as compared baseline ($p<0.01$) (Table 3 and Figure 11).

Table 1

Effects of a 2-hour placebo treatment on action potential characteristics in guinea pig papillary muscle

	RMP(mV)	APD(msec)	V_{max}(V/s)
Baseline	80 ± 4	155 ± 16	182 ± 28
Placebo (1 hr)	80 ± 3	157 ± 17	186 ± 28
Placebo (2 hrs) (n=4)	81 ± 3	159 ± 16	186 ± 30

Values represent mean ± SD

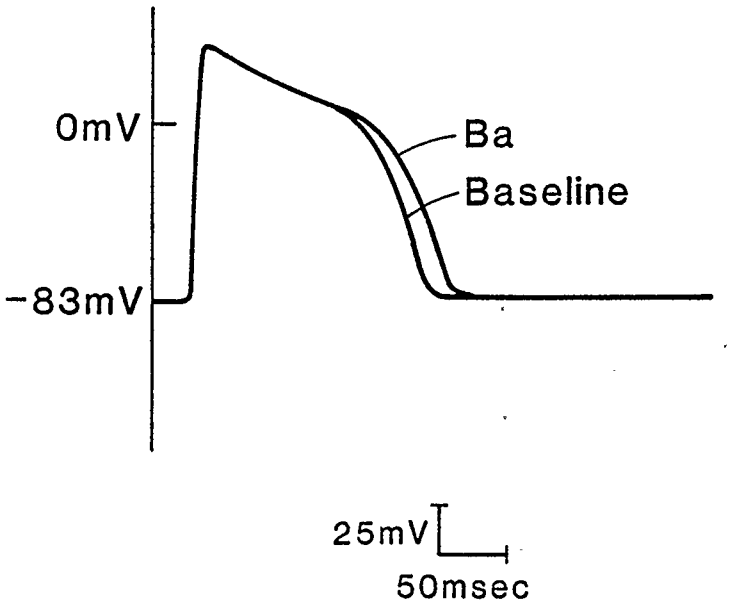

Fig. 10 Effect of barium chloride (10^{-5} M) on the action potential was recorded from guinea pig papillary muscle stimulated at basic cycle lengths of 500 msec at 37°C.

In contrast, when mexiletine was combined with either O-demethyl-encainide or barium chloride, a trend towards a shortening of action potential duration (3-5 msec) was seen. However, neither of these combinations significantly shortened refractoriness, resulting in an increase in the ratio of effective refractory period and action potential duration (Table 3 and Figure 11).

Both O-demethyl-encainide and mexiletine significantly depressed steady state V_{max} (from 176 ± 22 V/s at baseline to 135 ± 11 V/s with O-demethyl-encainide, $p< 0.05$; and from 195 ± 29 V/s at baseline to 180 ± 26 V/s with mexiletine, $p<0.05$) (Table 2). The combination of O-demethyl-encainide and mexiletine produced a significantly greater reduction in steady-state V_{max} from 135 ± 11 (V/s) with O-demethyl-encainide to 123 ± 13 (V/s) alone with the two drugs in combination ($p<0.01$). While barium chloride alone did not have any significant effect on V_{max}, the combination of barium chloride and mexiletine produced a significantly greater reduction in steady-state V_{max} than mexiletine alone (from 180 ± 26 V/s with mexiletine alone to 166 ± 18 V/s, $p<0.05$). Similarly, the addition of barium chloride to the combination of O-demethyl-encainide and mexiletine decreased steady- state V_{max} to 114 ± 14 (V/s), which was significantly greater than any single or two-drug combinations ($p< 0.05$) (Table 2). However, this enhanced depression of steady state V_{max} produced by barium chloride in combination with mexiletine and O-demethyl-encainide was not observed with the combination of O-demethyl-encainide and barium chloride.

Table 2

Steady state effects of O-demethyl-encainide, mexiletine, barium chloride and their combinations on action potential characteristics in guinea pig papillary muscle

	RMP(mV)	APD(msec)	Vmax(V/s)	VERP(msec)
DF	-84 ± 2	181 ± 14	176 ± 22	181 ± 19
ODME	-85 ± 2	187 ± 15 *	135 ± 11 *	189 ± 18 *
ODME+Mex	-85 ± 2	183 ± 11	123 ± 13 *	191 ± 19
ODME+Mex+Ba	-85 ± 2	200 ± 12**	114 ± 14**	207 ± 18**
(n=5)				
DF	-84 ± 3	174 ± 13	179 ± 17	172 ± 13
ODME	-84 ± 2	180 ± 15 *	133 ± 15**	181 ± 13**
ODME+Ba	-85 ± 3	201 ± 15**	129 ± 20**	202 ± 13**
ODME+Ba+Mex	-84 ± 3	197 ± 12**	109 ± 17**	202 ± 12**
(n=6)				
DF	-83 ± 2	190 ± 14	195 ± 29	189 ± 19
Mex	-84 ± 3	185 ± 13 *	180 ± 26 *	187 ± 16
Mex+Ba	-84 ± 3	207 ± 15*	166 ± 18 *	206 ± 18**
(n=5)				
DF	-82 ± 2	167 ± 16	144 ± 17	169 ± 21
Ba	-83 ± 2	187 ± 16**	141 ± 22	186 ± 22**
(n=5)				

DF designates drug free

ODME designates O-demethyl-encainide (3×10^{-7}M)

DF designates drug free

ODME designates O-demethyl-encainide (3×10^{-7} M)

Mex designates mexiletine (4×10^{-6} M)

Ba designates barium chloride (10^{-5} M)

RMP represents resting membrane potential

APD represents action potential duration

V_{max} represents the maximum upstroke velocity of the action potential

VERP represents ventricular effective refractory period

Values represent mean $\pm$ SD

* significantly different from DF, $p < 0.05$

** significantly different from DF, $p < 0.01$

Table 3

Comparison of the changes in the action potential characteristics by O-demethyl-encainide, mexiletine, barium chloride and their combinations in guinea pig papillary muscle

	Δ RMP(mV)	Δ APD(msec)	Δ Vmax(V/s)	Δ VERP(msec)
ODME	0.5 ± 1	5 ± 3	-40 ± 25	8 ± 4
ODME+Mex	0.8 ± 1	2 ± 6	-52 ± 25**	10 ± 7
ODME+Mex+Ba	0.3 ± 1	18 ± 5** (**)	-62 ± 26*** (**)	26 ± 9** (**)
ODME	-0.3 ± 1	6 ± 5	-47 ± 11	9 ± 3
ODME+Ba	0.7 ± 1	28 ± 5**	-50 ± 17	30 ± 6**
ODME+Ba+Mex	-0.5 ± 1	23 ± 2** (*)	-67 ± 15** (**)	30 ± 6**
Mex	0.6 ± 1	-5 ± 3	-15 ± 14	-3 ± 6
Mex+Ba	1 ± 1	17 ± 4 (**)	-30 ± 22 (*)	17 ± 5 (**)
Ba	0.8 ± 2	20 ± 4	-3 ± 12	17 ± 3

Values represent mean ± SD

Δ represents difference from baseline.

* significantly different from single drug treatment, $p < 0.05$

** significantly different from single drug treatment, $p < 0.01$

*** significantly different from single drug treatment, $p < 0.001$

A.

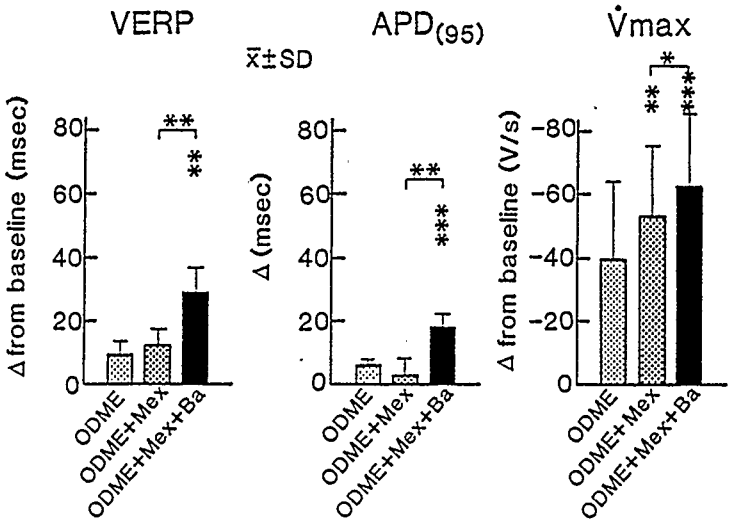
VERP
APD(95)
V̇max
x̄±SD
Δ from baseline (msec)
Δ (msec)
Δ from baseline (V/s)
ODME
ODME+Mex
ODME+Mex+Ba

B.

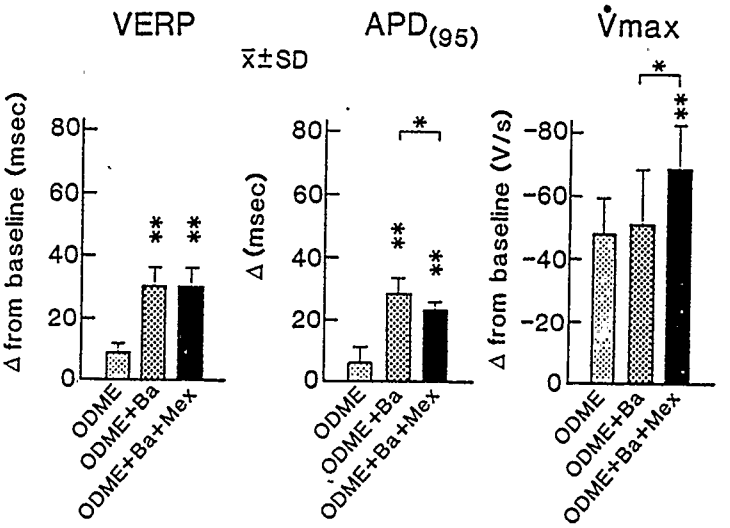
VERP
APD(95)
V̇max
x̄±SD
Δ from baseline (msec)
Δ (msec)
Δ from baseline (V/s)
ODME
ODME+Ba
ODME+Ba+Mex

C.

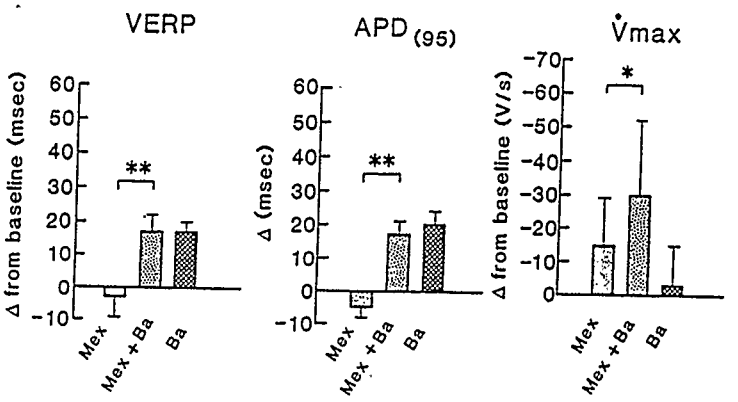
VERP
APD (95)
V̇max
Δ from baseline (msec)
Δ (msec)
Δ from baseline (V/s)
Mex
Mex +Ba
Ba

Fig. 11 A. Effects of O-demethyl-encainide, the combination of O-demethyl-encainide and mexiletine and the combination of O-demethyl-encainide, mexiletine and barium chloride on refractoriness, action potential duration and steady-state V_{max}. B. Effects of O-demethyl-encainide, the combination of O-demethyl-encainide and barium chloride and the combination of O-demethyl-encainide, barium chloride and mexiletine on the refractoriness, action potential duration and steady-state V_{max}. C. Effects of mexiletine and the combination of mexiletine and barium chloride on refractoriness, action potential duration and steady-state V_{max}. The combination of O-demethyl-encainide and mexiletine produced an additive decrease in V_{max}. The addition of barium chloride to mexiletine produced a synergistic decrease in V_{max}. However, the addition of barium chloride to O-demethyl-encainide did not produce the synergistic effect on V_{max}.

4.2 Use-Dependent Decrease in V_{max}

After a prolonged rest period, a train of stimuli at a cycle length of 500 msec produced a progressive decrease in V_{max} to a steady-state level. The magnitude of this decrease, expressed as a percentage of the initial value of V_{max} (the first beat after the pause), was termed the percentage of use-dependent block. In this study, there were no significant changes in V_{max} during the stimulation train in the drug free state. In contrast, O-demethyl-encainide produced a modest but significant use-dependent block of V_{max} of 9 ± 1%. When mexiletine was combined with O-demethyl-encainide, a significantly greater use-dependent block of 16 ± 3% was observed ($p< 0.05$) as compared to O-demethyl-encainide alone. While barium chloride had no effect on V_{max}, the addition of barium chloride to the combination of O-demethyl-encainide and mexiletine produced a further increase in use-dependent block of 20 ± 2% ($p< 0.05$), as compared to the combination of O-demethyl-encainide and mexiletine (Figure 12). Similarly, the combination of mexiletine and barium chloride produced a significantly greater use-dependent block (11 ± 3%) compared to mexiletine alone (7 ± 4%, $p< 0.05$) (Figure 13). However, there was no difference in the degree of use-dependent block between O-demethyl-encainide alone (13 ± 3%) and the combination of O-demethyl-encainide and barium chloride (14 ± 2%) (Figure 14). The mean percent changes in use-dependent block are summarized in Table 4.

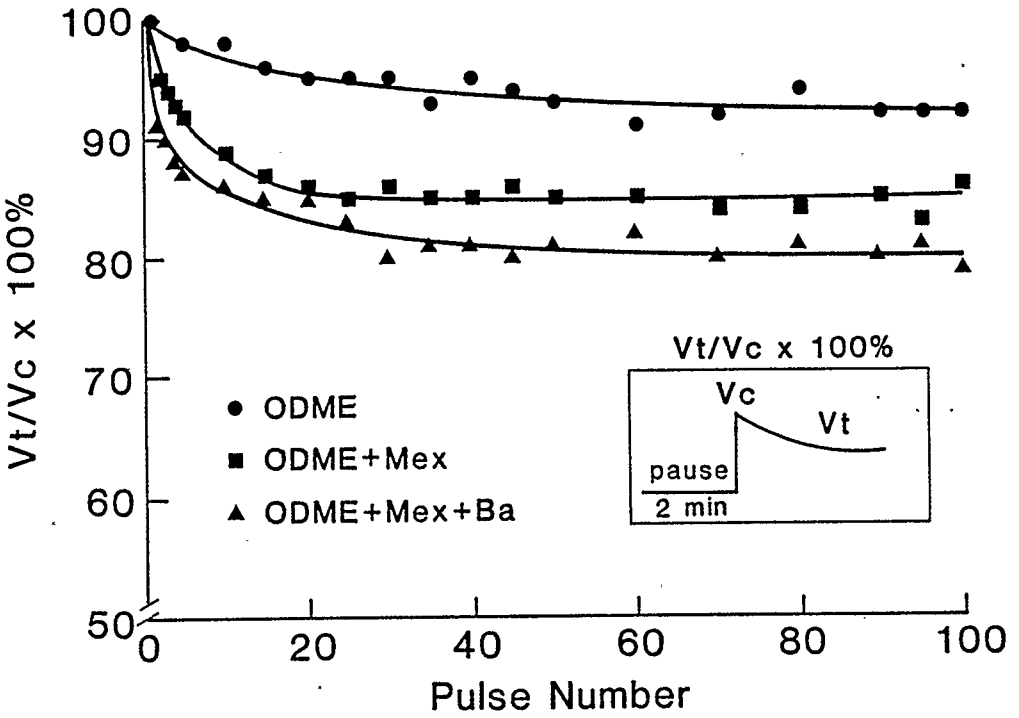

Fig. 12 Use-dependent decrease in V_{max} obtained in the presence of O-demethyl-encainide (3×10^{-7}M), the combination of O-demethyl-encainide and mexiletine (4×10^{-6}M), and combination of O-demethyl-encainide, mexiletine and barium chloride (10^{-5}M) at pacing cycle length of 500 msec after a rest period of 2 min. Vc = V_{max} of the first pulse of the train after a 2 min rest period. Vt = V_{max} of the rest of the pulses of the train. The ratio of Vt/Vc was then plotted as a percent change as function of the pulse number. O-demethyl-encainide alone and the combination of O-demethyl-encainide and mexiletine were single exponential curve fitting. The combination of O-demethyl-encainide, mexiletine and barium chloride was biexponential curve fitting. For τ values see Table 4.

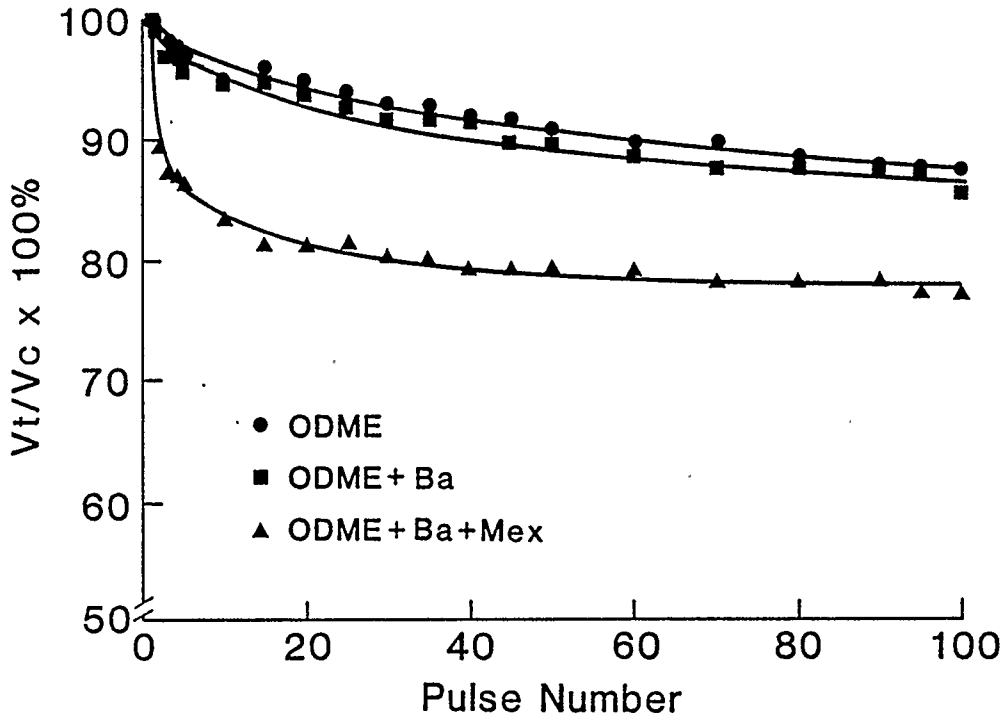

Fig. 13 Use-dependent decrease in V_{max} obtained in the presence of 0-demethyl-encainide (3×10^{-7}M), the combination of 0-demethyl-encainide and barium chloride (10^{-5}M), and the combination of 0-demethyl-encainide, barium chloride and mexiletine (4×10^{-6}M) at pacing cycle length of 500 msec after a rest period of 2 min. Vc = V_{max} of the first pulse of the train after a 2 min rest period. Vt = V_{max} of the rest of the pulses of the train. The ratio of Vt/Vc was then plotted as a percent change as function of the pulse number. 0-demethyl-encainide and the combination of 0-demethyl-encainide and barium chloride were single exponential curve fitting. The combination of combination of 0-demethyl-encainide, barium chloride and mexiletine was biexponential curve fitting. For τ values see Table 4.

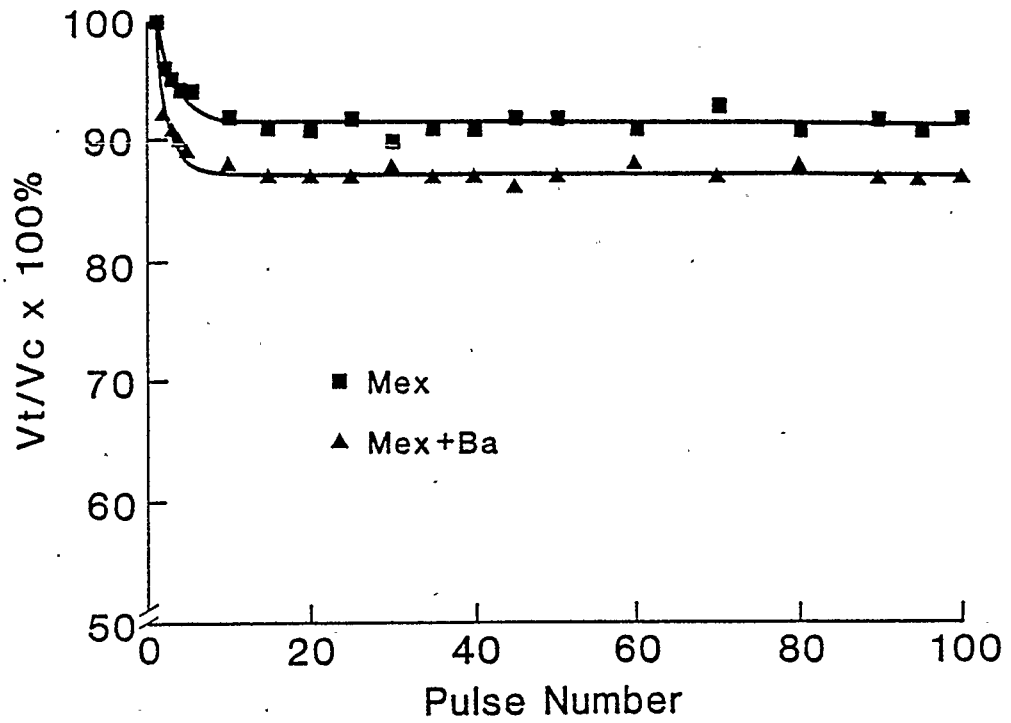

Fig. 14 Use-dependent decrease in V_{max} obtained in the presence of mexiletine (4×10^{-6}M), and the combination of mexiletine and barium chloride (10^{-5}M) at pacing cycle length of 500 msec after a rest period of 2 min. Vc = V_{max} of the first pulse of the train after a 2 min rest period. Vt = V_{max} of the rest of pulses of the train. The ratio of Vt/Vc was then plotted as a percent change as function of the pulse number. The data from both mexiletine and the combination of mexiletine and barium chloride were single exponential curve fitting. For τ values see Table 4.

4.3 Onset Kinetics of Use-Dependent Decrease in V_{max}

The onset kinetics of use-dependent block were defined by fitting the data to an equation with a single exponential term:

$$V_t / V_c\ (\%) = A + A_1 \exp[(-p)/\tau]$$

or a biexponential equation:

$$V_t / V_c\ (\%) = A + A_f \exp[(-p)/\tau_f] + A_s \exp[(-p)/\tau_s]$$

to calculate the time constants (τ or τ_f and τ_s). V_c and V_t represent the V_{max} of the first beat after the pause and V_{max} of other beats in the train (the test beats) respectively; A represents the V_{max} at steady state as the percentage of V_c ; A_1 represents the percentage of the use-dependent decrease in V_{max} and τ is the time constant of the onset of use-dependent decrease in V_{max} expressed in term of the pulse number. P represents the pulse number. In biexponential equation, A_f and A_s represent the percentage of the use-dependent decrease in V_{max} of the fast and slow components and τ_f and τ_s are the time constants of the onset of use-dependent decrease in V_{max} of the fast and slow components respectively.

The onset kinetics of O-demethyl-encainide, mexiletine, and the combination of O-demethyl-encainide and barium chloride as well as the combination of mexiletine and barium chloride, were fitted by a single

exponential curve. Onset time constants are 39 ± 15 pulses for O-demethyl-encainide and 36 ± 18 pulses for the combination of O-demethyl-encainide and barium chloride, which is not significantly different from O-demethyl-encainide (Table 4). The onset time constant was 4 ± 2 pulses for mexiletine alone, which was not significantly different from the combination of mexiletine and barium chloride (2 ± 1 pulse). The results from the combination of O-demethyl-encainide and mexiletine were fit to a single exponential equation. The time constant was 6 ± 2 pulses, which was much faster than that seen with O-demethyl-encainide alone (39 ± 15 pulses) ($p<0.01$). In addition, two experiments of combination of O-demethyl-encainide and mexiletine were also fit to a biexponential equation. When barium chloride was added to the combination of O-demethyl-encainide and mexiletine, the onset kinetics of use-dependent block became biexponential. The τ_f was 0.5 ± 0.1 (pulse) and τ_s was 18 ± 7 (pulses) (Table 4).

Table 4

Comparison of the extent of use-dependent block (UDB) and onset time constants of UDB seen with the single drugs and with drug combinations

	UDB(%)	τ #	τ_f #	τ_s #
ODME	9 ± 1	36 ± 12		
ODME+Mex	16 ± 3*	6 ± 2**		
ODME+Mex+Ba	20 ± 2** *		0.5 ± 0.1	18 ± 7
ODME	13 ± 3	39 ± 15		
ODME+Ba	14 ± 2	36 ± 18		
ODME+Ba+Mex	22 ± 4* *		0.8 ± 0.4	23 ± 11
Mex	8 ± 4	4 ± 2		
Mex+Ba	11 ± 3*	2 ± 1		

#: The τ is the time constant of use-dependent block expressed in terms of the pulse number. The τ_f and τ_s are the time constants of use-dependent block for the biexponential curve fitting.

ODME designates O-demethyl-encainide (3×10^{-7} M).

Mex designates mexiletine (4×10^{-6} M).

Ba designates barium chloride (10^{-5} M).

* significantly different from single drug treatment, $p < 0.05$

** significantly different from single drug treatment, $p<0.01$

4.4 Recovery of V_{max} from Use-Dependent Block

The rate at which V_{max} recovered after an imposed train of stimuli was studied by adding single extrastimulus at varying intervals after a series of trains of stimuli at a constant frequency (cycle length of 500 msec). In order to quantitate these kinetics of recovery from use-dependent block, it was necessary to use higher concentrations of O-demethyl-encainide (1.5×10^{-6}M). The data were fit to a single exponential equation:

$$V_{max_t} / V_{max_c} (\%) = 100 - A \exp[(-t)/\tau]$$

or a biexponential equation:

$$V_{max_t} / V_{max_c} (\%) = 100 - A_f \exp[(-t)/\tau_f] - A_s \exp[(-t)/\tau_s]$$

Where V_{max_c} is the V_{max} of the first beat after a 2-min pause, V_{max_t} represents the V_{max} of the extrastimuli after a variable rest period (S_1-S_2 interval). A, A_f and A_s are constants. $A = 100 - V_{max_o}/V_{max_c}$ when $V_{max_o} = V_{max}$ at t=0 (in the single exponential equation) and $A_f + A_s = 100 - V_{max_o}/V_{max_c}$ when $V_{max_o} = V_{max}$ at t=0 (in the biexponential equation). Figure 15 shows the time course of the recovery from O-demethyl-encainide and mexiletine, and that of the recovery from the combination of O-demethyl-encainide, mexiletine, and

barium chloride. The best-fit data are shown in Table 5. O-demethyl-encainide resulted in a single exponential recovery time course with a time constant of recovery of 8080 ± 1520 msec. Mexiletine also exhibited a single exponential recovery time course with a time constant of 362 ± 71 msec, which was much faster than that seen with O-demethyl-encainide. When mexiletine was added to O-demethyl-encainide, the recovery process was best fit by a biexponential process with τ_f of 287 ± 32 msec and τ_s of 8120 ± 1450 msec. The τ_f of the combination was therefore similar to the mexiletine data, and the τ_s was similar to O-demethyl-encainide. As can be seen in Table 5, the addition of barium chloride to the combination of O-demethyl-encainide and mexiletine did not significantly alter this biexponential time course. The τ_f was 303 ± 16 msec and τ_s was 9430 ± 2420 msec. Similarly, adding barium chloride to mexiletine did not significantly alter the time course of recovery from mexiletine-induced use-dependent block (295 ± 165 msec), although the percentage of use-dependent decrease in v_{max} produced by the combination of mexiletine and barium chloride was significantly greater than that produced by mexiletine alone.

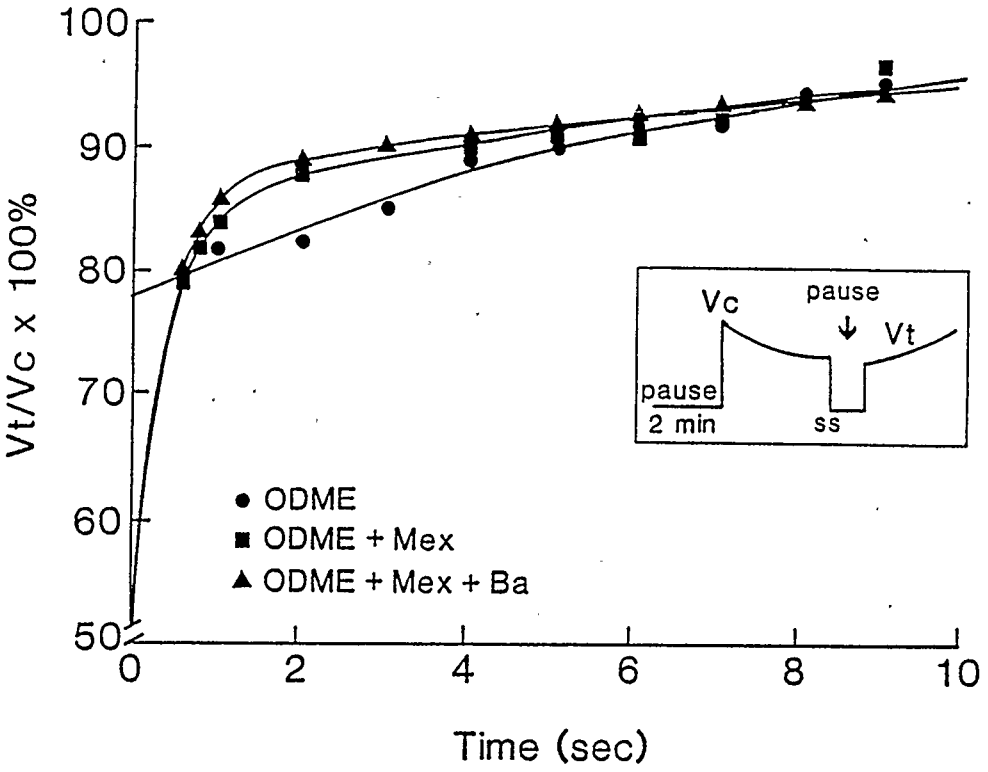

Fig. 15 Effects of O-demethyl-encainide (1.5×10^{-6}M), the combination of O-demethyl-encainide and mexiletine (4×10^{-6}M), and the combination of O-demethyl-encainide, mexiletine and barium chloride (10^{-5}M) on the recovery of V_{max} were assessed by 85-pulse trains of action potentials at pacing cycle length of 500 msec, followed by a variable rest period (S_1-S_2 interval, from 600 - 9000 msec). In O-demethyl-encainide V_{max} had a single exponential recovery time course. The combination of O-demethyl-encainide and mexiletine had biexponential curve fitting and addition of barium chloride to this combination did not alter this biexponential recovery process. For τ values see Table 5.

Table 5

Comparison of recovery kinetics with the drugs alone and in combination

	τ (msec)	τ_f (msec)	τ_s (msec)
ODME	8080 ± 1520		
ODME+Mex		288 ± 32	8120 ± 1450
ODME+Mex+Ba		303 ± 16	9430 ± 2420
(n=4)			
Mex	362 ± 71		
Mex+Ba	295 ± 165		
(n=3)			

Values represent mean ± SD

ODME designates O-demethyl-encainide (1.5×10^{-6} M).

Mex designates mexiletine (4×10^{-6} M).

Ba designates barium chloride (10^{-5} M).

τ designates recovery time constant from use-dependent block

τ_f and τ_s designate recovery time constants from use-dependent block for the biexponential curve fitting.

4.5 Tonic Decrease in V_{max}

Tonic block was defined as the decrease of V_{max} of the first action potential after a prolonged rest period. In this study, O-demethyl-encainide and mexiletine induced 12 ± 6 % and 4 ± 5% tonic block, respectively. The addition of mexiletine to O-demethyl-encainide produced a significant increase in the extent of tonic block (15 ± 8%, $p<0.05$) compared to that seen with O-demethyl-encainide alone. The addition of barium chloride did not significantly change the amount of tonic block produced by any drug treatment.

CHAPTER 5

DISCUSSION

5.1 Experimental Design

The experimental design used in this study has some advantages. First, the agents chosen for the experiments produced relatively selective electrophysiologic effects. Barium chloride in low concentrations selectively prolonged action potential duration with no effects on resting membrane potential or V_{max}. O-demethyl-encainide produced a use-dependent decrease in V_{max} with slow onset-offset kinetics. Mexiletine produced a use-dependent decrease in V_{max} with fast onset-offset kinetics. Secondly, the concentrations of agents used in this study are in the clinical therapeutic range. Thirdly, the experiments were performed at physiologic temperatures. It has been shown that temperature can affect both the kinetics of sodium current activation and inactivation (72,73), as well as the interaction of sodium channel blockers with sodium channels. Therefore, the electrophysiologic data obtained from this study are relevant to the clinical situations. Finally, both ventricular refractoriness and V_{max} were measured in this study. The majority of other conventional microelectrode studies did not measure refractoriness.

5.2 Comparison of Our Results with Previous Work

A number of other studies have examined the electrophysiologic effects of the drugs used in the present investigation. Johns et al reported that O-demethyl-encainide was a potent blocker of the activated cardiac sodium channels with little or no effect on the inactivated sodium channels (70). The kinetics of recovery from use-dependent block of O-demethyl-encainide was very sensitive to changes in temperature and voltage. In the study of Johns et al, there was no recovery of the sodium current up to 10 min after the pacing trains at 20°C. However, at 35°C, the time constant of recovery was 25 ± 5 sec. The time constant of recovery from use-dependent block produced by O-demethyl-encainide in the present study was 8.1 ± 1.5 sec measured at 37°C. The difference in recovery time constant between the two studies may result from the difference in the temperature used, as well as the difference in the resting membrane potentials. The resting membrane potentials in this study were -85 ± 2 mV but in the study of Johns et al, the holding potential was -100 mV.

It is known that barium chloride at low concentrations (1-500 μM) is a potent and quite selective blocker of I_{K1} (68,69). However, in canine myocytes a concentration of 50 μM of barium chloride produced 3 to 4 mV of depolarization (69). In order to avoid this depolarization, we used a lower concentration of barium chloride (10 μM) which selectively prolonged the action potential without changing the resting membrane potential and V_{max}.

A number of previous studies have examined the electrophysiologic effects of mexiletine (74,75). The effects of mexiletine in the present study were comparable to those previously reported. Mexiletine produced use-dependent depression of V_{max} with fast onset/offset kinetics. The presence of TTX-sensitive "window current" in guinea pig ventricle remains controversial. Hume et al (76) and Mitchell et al (77) reported that a TTX-sensitive steady sodium current (window current) was absent in guinea pig ventricle myocytes. However, more recently Kiyosue et al (78) have obtained evidence for the presence of a small but significant TTX-sensitive "window current". They have postulated that this current may play a role in maintaining the action potential plateau and duration in guinea pig ventricle myocytes. Therefore, the slight shortening of the action potential duration produced by mexiletine may be caused by blockade of this "window current" or by blockade of other ionic currents underlying the plateau, such as calcium current (79).

Other investigators have studied interactions between sodium channel blockers and drugs which prolong repolarization. Stroobandt et al assessed the interaction between sotalol and aprindine (80). The combination of sotalol and aprindine produced an increase in use-dependent block, tonic block and steady-state decrease in V_{max}. However, in that study supra-physiologic concentrations of sotalol (10^{-4}M) were used, which produced sodium channel blockade in addition to prolonging repolarization.

A number of previous publications have studied interaction between class Ic and class Ib drugs. Kohlhardt et al (81) and Valenzuela et al (65) examined the interaction between propafenone (class Ic) and lidocaine (class Ib) in guinea pig papillary muscle. Low concentrations of lidocaine and propafenone in combination produced an increase in the total block (Kohlhardt et al) and a significant increase in the extent of use-dependent block of V_{max} (Valenzuela et al). Recently, Valenzuela et al (82) have studied the combination of flecainide (class Ic) and mexiletine (class Ib). They found that this combination synergistically increased the magnitude and the onset rate of the V_{max} block at driving rates faster than 0.5 Hz. The results in the present study with the combination of O-demethyl-encainide (class Ic) and mexiletine are similar to those produced by the propafenone-lidocaine combination as well as by the flecainide-mexiletine combination. The O-demethyl-encainide and mexiletine combination produced a statistically significant increase in both total block and the extent of use-dependent block, compared to O-demethyl-encainide alone. Furthermore, this study shows that the addition of barium chloride to the combination of O-demethyl-encainide and mexiletine caused a significant increase in the extent of use-dependent block with a faster time constant for the onset of the block without a significant change in the recovery kinetics (figures 12,15) (Tables 4, 5)

5.3 New Findings

The new information provided by this work includes: 1) The demonstration that combination of O-demethyl-encainide, mexiletine and barium chloride produced lengthening of ventricular effective refractory period which was significantly greater than that seen with any single drug treatment or either of the combinations: O-demethyl-encainide and mexiletine; or mexiletine and barium chloride. This increase in refractoriness was likely caused by a prolongation of the action potential. 2) While barium chloride does not have any effect on V_{max}, the combination of mexiletine and barium chloride produced a synergistic depression of the steady state V_{max} than mexiletine alone. Similarly, the combination of O-demethyl-encainide, mexiletine and barium chloride produced a greater decrease in V_{max} than that seen with any single drug or drug combinations used in this study. 3) The addition of barium chloride to mexiletine significantly increased the extent of use-dependent block. Similarly, barium chloride combined with O-demethyl-encainide and mexiletine also induced a significantly greater amount of use-dependent block than the two drug combination, and the onset kinetics of use-dependent block of this combination showed a biexponential time course.

5.4 Possible Mechanisms of Drug Interactions

According to conventional HH theory, sodium channels cycle through the rested, activated and inactivated states during each action potential. Most antiarrhythmic agents have a very low affinity for the rested state, but a high affinity for either the activated or inactivated state (41). The modulated receptor hypothesis proposes that different rate constants characterize the association and dissociation of antiarrhythmic drugs to and from their binding sites, dependent on the state of the sodium channels. For a drug (e.g., O-demethyl-encainide, a blocker of activated sodium channel) with slow kinetics, the rate of the drug dissociation is slow enough so that a degree of residual sodium-channel block persists between beats. However, for a drug (e.g., mexiletine) with fast kinetics, block develops and dissipates rapidly during each action potential. The additive sodium channel block produced by the combination of O-demethyl- encainide and mexiletine may result from the summation of persistent block of the activated state induced by O-demethyl-encainide coupled with the block of the inactivated state induced by mexiletine. Thus, the interaction between sodium channel blockers which bind to the different channel states with slow and fast kinetics could be one mechanism of the enhanced electrophysiologic effect produced by the combination of O-demethyl-encainide and mexiletine.

In addition, as shown in Figure 4, activation and inactivation of the sodium channels were controlled by different regions of the sodium

channels. Therefore, the segment 4 of repeat I of the sodium channel responsible for the activation may modulate the binding of O-demethyl-encainide to the receptor and the loop between repeats III and IV of the sodium channel located on the cytoplasmic side may modulate the binding of mexiletine to the inactivated sodium channels.

It has been shown that the degree of use-dependent block produced by lidocaine increased as pulse durations were prolonged or holding potentials were depolarized in guinea pig ventricular myocytes (83). Action potential prolongation with barium chloride may be analogous to voltage clamping the cell at depolarized potentials for a longer time and therefore may result in an increased proportion of sodium channels being in the inactivated state (25). Since mexiletine, similar to lidocaine, preferentially binds to the inactivated sodium channel with fast kinetics, prolongation of the action potential may favor mexiletine interaction with inactivated sodium channels and modulate the extent of state-dependent drug interactions. In contrast, the combination of an activated sodium channel blocker (O-demethyl-encainide) and barium chloride did not further decrease V_{max} compared to O-demethyl-encainide alone, which implies that action potential prolongation may not modulate sodium channel blockade induced by activated sodium channel blockers.

The balance between block development during each action potential and recovery from block during the diastolic interval determines the maximum percentage of sodium channel block. As shown in Figure 16, for

a drug with certain recovery time constant, more block remains at the end of the shorter diastole (25). With the constant pacing cycle length in our study, action potential prolongation by barium chloride causes a shortening of the diastolic interval, which may result in less mexiletine dissociating from the binding sites and cause a greater block of the sodium channel. On the other hand, the recovery kinetics of sodium channels from the inactivated state to the rested state is strongly voltage-dependent. The Figure 17 shows the recovery time constant of sodium channel at -80 mV is 3.5 times faster than that at -70 mV (84). Prolongation of the final phase (at about -70 mV) of action potential by barium chloride may slow the sodium channel recovery from the inactivated state to the rested state and lead to a decrease in the number of sodium channels available for activation. As a result, the combination of a drug (e.g., barium chloride) which prolongs action potential duration and a drug (e.g., mexiletine) which preferentially binds to the inactivated sodium channel may lead to an increase in the degree of sodium channel block. Our results showed that the recovery time course of mexiletine followed a single exponential process. The addition of barium chloride to mexiletine did not alter the recovery time course. As mentioned above, prolongation of action potential duration by barium chloride is expected to slow the sodium channel recovery from the inactivated state. Since the effect of barium chloride on the action potential prolongation was relatively small (about 20 msec) and limitation of the approach we used for measuring the diastolic recovery interval, this change in recovery time

course produced by the combination of mexileitne and barium chloride was not detected in this study.

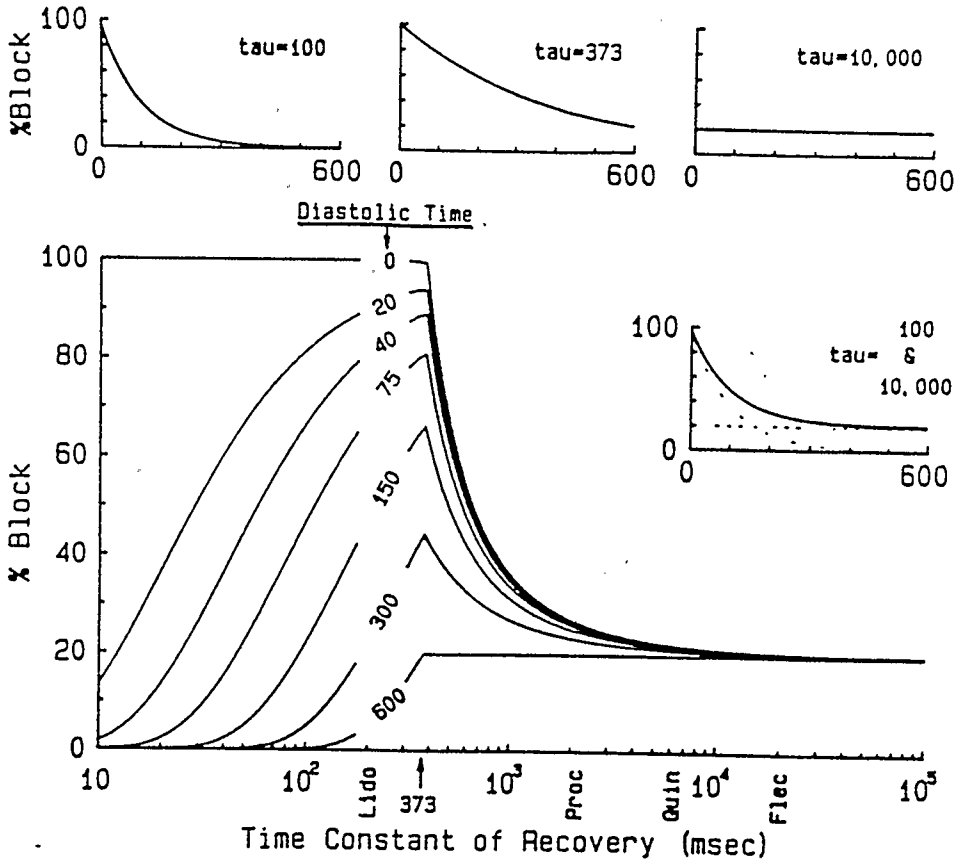
%Block
100
0
0
600
tau=100
tau=373
tau=10, 000
Diastolic Time
% Block
100
80
60
40
20
0
10
10^2
10^3
10^4
10^5
Lido
373
Proc
Quin
Flec
0
20
40
75
150
300
600
tau= 100 & 10, 000
Time Constant of Recovery (msec)

Fig. 16 Maximum block at beginning of diastole (curve labeled 0), at end of a 600 msec diastolic period results in no more than 20% block as a function of the time constant of recovery from block. For this maximum the block at diastolic times of 20, 40, 75, 150, 300, and 600 msec was also computed. On the abscissa time constants for lidocaine, procainamide, quinidine and flecainide in normal tissue are indicated. Under these conditions the most diastolic block is maintained for the longest possible time for the time constant of 373 msec (arrow on abscissa). The block as a function of diastolic time for this 373 msec time constant of recovery is plotted in the center top inset. The top left inset illustrates the time course of maximum diastolic block for a drug with 100 msec time constant of recovery, while the top right inset shows this for 10,000 msec time constant. The bottom inset shows the maximum block by the combination of two drugs (solid line) with time constants of 100 and 10,000 msec. Clearly the combination can achieve more diastolic block than each of the individual drugs of the combination (modified from Ref.25).

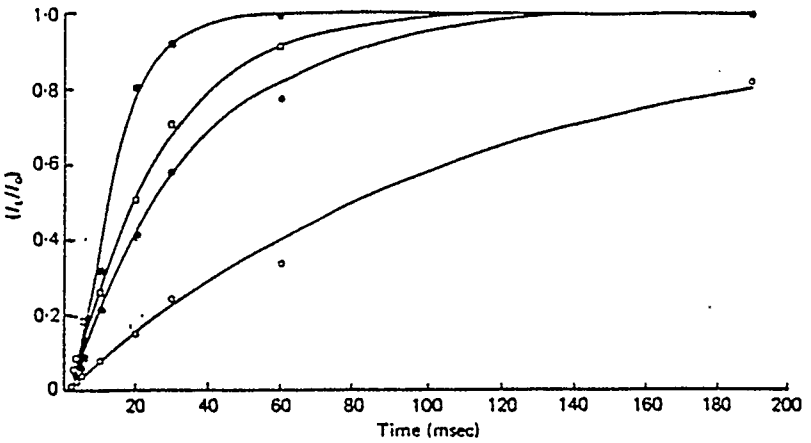

Fig. 17 Time course of recovery of the Na system from complete inactivation. Ordinate: I_t/I_o where I_t is test-pulse current at time t after end of the prepulse and I_o is prepulse current. Abscissa: time interval (t, msec) between end of the prepulse and onset of test pulse. Each curve represents recovery time course of I_{Na} from inactivation at baseline potentials of -70 (○), -80 (●), -90 (□) and -100 (■) mV. Lines drawn are best fit to exponential points and correspond to two exponential components with time constants τ_{r1} and τ_{r2}, which had the values 1.9 and 119 msec (-70 mV), 1.7 and 33 msec (-80 mV), 3.3 and 25 msec (-90 mV), and 3.9 and 10 msec(-100 mV) respectively (modified from Ref. 84).

5.5 Limitations

Our study has limitations. First, although the maximal upstroke velocity of the cardiac action potential has traditionally been used as an index of sodium channel availability (85), this parameter gives only the indirect information of g_{Na}. The original rationale for using V_{max} was based on the assumptions that 1) total ionic current at the time of V_{max} is dominated by I_{Na} and 2) at the time of V_{max}, I_{Na} is strictly proportional to the available g_{Na} just before the upstroke (5). However, several studies have shown that there is a nonlinear relation between V_{max} and I_{Na} (86,87). Therefore, V_{max} may not be a reliable method for quantitation of amount of sodium-channel blockade by antiarrhythmic drugs. Nevertheless, recent voltage clamp experiments by sheets et al (87) in single cardiac Purkinje cells have revealed that the non linearity between V_{max} and I_{Na} at 37°C is relatively small, and that it declines further with increasing temperature.

Secondly, experiments were performed in isolated papillary muscles rather than intact animal models. Therefore, this study did not directly measure antiarrhythmic efficacy. However, the inducibility of reentrant arrhythmias is thought to depend on the wavelength of the cardiac impulse (wavelength = conduction velocity x refractory period) (88). It has also been suggested that drugs that shorten the wavelength might be regarded as arrhythmogenic, whereas agents that increase the wavelength can be expected to possess antiarrhythmic

properties. Since a quadratic relationship exists between V_{max} and conduction velocity (89-92), V_{max} and ventricular effective refractory period obtained from our experiments may be relevant parameters for predicting antiarrhythmic efficacy.

Thirdly, some alternative agents were used instead of quinidine. The results may explain some phenomena produced by the combination of quinidine and mexiletine but may not be exactly the same. Quinidine has multiple electrophysiologic effects so that the combination of O-demethyl-encainide and barium chloride does not reproduce all the effects of quinidine.

Fourthly, antiarrhythmic drugs are applied to normal tissue in this study. Therefore, the effects observed in this study may be different if the drugs were used in the abnormal tissue.

Fifthly, It has been shown that in 20 mM HEPES buffered solution, the intracellular pH was close to that of the control solution. However, low concentration of HEPES buffered solution (5 mM) produced a small intracellular acidification (93). In our study, 10 mM HEPES buffered solution was used.

5.6 Clinical Relevance

Results from the present study may help explain the mechanisms of the enhanced antiarrhythmic efficacy produced by the combination of

quinidine and mexiletine observed in clinical setting. The supra-additive effects produced by the combination of quinidine and mexiletine may result from the summation of the persistent activated state sodium channel block coupled with inactivated state block, as well as an increase in the opportunity of mexiletine interaction with inactivated sodium channels due to prolongation of the action potential induced by quinidine. A greater blockade of the sodium channels may be expected from the combination of quinidine and mexiletine in depolarized tissue or during tachycardias since depolarization usually occurs in the damaged tissue which results in more sodium channels being in the inactivated state.

Ventricular tachycardia and ventricular fibrillation are leading causes of sudden cardiac death. The pharmacologic therapy of these arrhythmias has seen progress in recent years. However, the results of the Cardiac Arrhythmia Suppression Trial (CAST) have revealed that sodium-channel blockers do not have uniform efficacy or safety and suppression of premature ventricular depolarizations does not decrease mortality (40). Therefore, appropriate combination of drugs with differing electrophysiologic properties may improve therapeutic success of single drug. The present results may have implications for a rational selection of the combination of antiarrhythmic agents. For example, the combination of an inactivated sodium-channel blocker with an agent which prolongs the action potential may modulate the sodium-channel blockade and produce greater depression of V_{max} and prolongation of refractoriness.

CHAPTER 6

CONCLUSIONS

As described in Chapter 1, Class I antiarrhythmic agents have state-dependent association and dissociation rate constants to their binding site(s) on cardiac sodium channels. In addition to sodium channel blockade, Class Ia drugs can also prolong the action potential by blocking potassium channels. It has been shown that the combination of an agent with fast kinetics and an agent with slow kinetics can enhance antiarrhythmic efficacy in several animal models and in patients. However, it is unknown whether the prolongation of the action potential by blockade of potassium currents plays a role in the enhanced efficacy produced by the combination.

In this study, barium chloride was used in an attempt to determine the role of action potential prolongation in the enhanced electrophysiologic effects produced by the combination of selected sodium-channel blockers. Even though barium chloride alone did not have any effect on V_{max}, the combination of mexiletine (a blocker of the inactivated sodium channels) and barium chloride produced a synergistic depression of the steady-state V_{max} and an increase in the extent of use-dependent block as compared to mexiletine alone. Similar results were observed with addition of barium chloride to the combination of O-demethyl-encainide and mexiletine. However, no synergistic effect on the reduction in V_{max} was observed when barium chloride was

combined with O-demethyl-encainide (a blocker of the activated sodium channels).

The data from this work support a number of mechanisms for the enhanced electrophysiologic effects of the combination of O-demethyl-encainide, mexiletine and barium chloride. The additive sodium channel block produced by the combination of O-demethyl-encainide and mexiletine may result from the summation of persistent block of the activated state induced by a low concentration of O-demethyl-encainide with slow kinetics coupled with the block of the inactivated state with fast kinetics induced by mexiletine.

The mechanisms of these greater electrophysiologic effects produced by the combinations of sodium channel blockers and barium chloride are associated with the interaction between action potential prolongation by barium chloride and the inactivated sodium channel blockade induced by mexiletine. The prolongation of the action potential may be analogous to voltage clamping the cell at depolarized potentials for a longer time, therefore, resulting in an increased proportion of the sodium channel being in the inactivated state, which may favor mexiletine blockade of sodium channels. On the other hand, action potential prolongation causes a shortening of diastolic interval, which results in less mexiletine dissociating from the binding sites and therefore modulates the degree of the sodium channel blockade. The results from present study suggest that prolongation of action potential duration plays an important role in the enhanced

antiarrhythmic efficacy by the combination of mexiletine and quinidine.

REFERENCES

1. Rosen MR, Hordof AJ: Mechanisms of arrhythmias. In: Roberts NK and H Gelband., eds. Cardiac Arrhythmias in the Neonate, Infant and Child. Appleton-Century-Crofts. New York, pp 111-131, 1977.
2. Katz AM, Messineo FC, Herbette L: Ion channels in membranes. Circulation 65 (Suppl I): 2-10, 1982.
3. Giles WR: Intracellular electrical activity in the heart. In: Patton HD, Fuchs AF, Hille B, Scher AM, Steiner R,. eds. Textbook of Physiology. Philadelphia, W.B. Saunders, Vol. 2 pp 782-795, 1989.
4. Noble D: Ionic basis of rhythmic activity in the heart. In: Zipes DP, Jalife J., eds. Cardiac Electrophysiology and Arrhythmias. New York, Grune and Stratton, pp 3-7, 1985.
5. Tsien RW, Siegelbaum SA: Excitable tissues: The Heart. In: Andreoli TE, Hoffman JF, Fanestil DD., eds. Physiology of Membrane Disorders. New York, Plenum Press, pp 517-518, 1978.
6. Kirsch GE, Brown AM: Molecular bases and single-channel activity: Cardiac sodium channels. In: Zipes DP and Jalife J eds., Cardiac Electrophysiology from Cell-to-Bedside. Philadelphia, W. B. Saunders, Co. pp 1-10, 1990.
7. Shibata EF, Drury T, Refsum H, Aldrete V, Giles WR: A transient outward current in human atrium. Am. J. Physiol. 257: H1773-H1781, 1989.

8. Imaizumi Y, Giles WR: Quinidine-induced inhibition of a transient outward current in cardiac muscle. Am. J. Physiol. 253: H704-H708, 1987.

9. Gilmour RF, Salata JJ, Davis JR: Effect of 4-aminopyridine on rate related depression of cardiac action potentials. Am. J. Physiol. 251: H297-H306, 1986.

10. Kenyon JL, Gibbons WR: 4-Aminopyridine and the early outward current of sheep cardiac Purkinje fibers. J. Gen. Physiol. 73: 139-157, 1979.

11. Kenyon JL, Sutko JL: Calcium- and voltage- activated plateau currents of cardiac Purkinje fibers. J. Gen. Physiol. 89: 921-958, 1987.

12. Kukushkin NI, Gainullin RZ, Sosunov EA: Transient outward current and rate dependence of action potential duration in rabbit cardiac ventricular muscle. Pflugers Arch. 399: 87-92, 1983.

13. Watanabe T, Delbridge LM, Bustamante JO, McDonald TF: Heterogeneity of the action potential in isolated rat ventricular myocytes and tissue. Circ. Res. 52: 280-290, 1983.

14. Tseng GN, Hoffman BF: Two components of transient outward current in canine ventricular myocytes. Circ. Res. 64: 633-647, 1989.

15. Beeler GW, Reuter H: Reconstruction of the action potential of ventricular myocardial fibers. J. Physiol. 268: 177-210, 1977.

16. Hiraoka M, Kawano S: Calcium-sensitive and insensitive transient outward current in rabbit ventricular myocytes. J. Physiol. 410: 187-212, 1989.

17. McDonald TF: The slow inward calcium current in the heart. Ann. Rev. Physiol. 44: 425-433, 1982.

18. Attwell D, Cohen I, Eisner D, Ohba M, Ojeda C: The steady-state TTX-sensitive ("window") sodium current in cardiac Purkinje fibers. Pflugers Arch. 379: 137-142, 1979.

19. Colatsky TJ, Gadsby DC: Is tetrodotoxin block of background sodium channel in canine cardiac Purkinje fibers voltage-dependent? J. Physiol. 306: 20p, 1980. (abstract)

20. Coraboeuf E, Deroubaix E, Coulombe A: Effect of tetrodotoxin on action potentials of the conducting system in the dog heart. Am. J. Physiol. 236: H561-H567, 1979.

21. Pennefather P, Cohen IS: Molecular mechanisms of cardiac K^+-channel regulation. In: Zipes DP and Jalife J., eds. Cardiac Electrophysiology from Cell-to-Bedside. Philadelphia, W. B. Saunders Co. pp 17-27, 1990.

22. Cohen IS, Kline R: Potassium fluctuations in the extracellular spaces of cardiac muscle. Evidence from the voltage-clamp and extracellular patassium selective microelectrodes. Circ. Res. 50: 1-6, 1982

23. Kline R, Cohen IS: Extracellular $[K^+]$ fluctuation in voltage-clamped canine cardiac Purkinje fibers. Biophys. J. 49: 663-668, 1984.

24. Hodgkin AL, Huxley AF: A quantitative description of membrane current and its application to conduction and excitation in nerve. J. Physiol. 117: 500-549, 1952.

25. Hondeghem LM: Antiarrhythmic agents: Modulated receptor applications. Circulation 75: 514-520, 1987.

26. Armstrong CM, Bezanilla F: Charge movement associated with the opening and closing of the activation gates of the Na channels. J. Gen. Physiol. 63: 533-552, 1974.

27. Armstrong CM, Bezanilla F: Inactivation of the sodium channel: Gating current experiments. J. Gen. Physiol. 70: 567-590, 1977.

28. Armstrong CM: Sodium channels and gating currents. Physiol. Rev. 61: 644-683, 1981.

29. Fozzard HA: Cardiac sodium channel kinetics. In: Samuel S, Beyar R, Kleber AG., eds. Cardiac Electrophysiology, Circulation, and Transport. Massachusetts, Kluwer Academic Publishers, pp 137-144, 1991.

30. Aldrich RW, Corey DP, Stevens CF: A reinterpretation of mammalian sodium channel gating based on single channel recording. Nature. 306: 436-441, 1983.

31. Kunze DL, Lacerda AE, Wilson DL: Cardiac Na currents and the inactivating reopening and waiting properties of single cardiac Na channels. J. Gen. Physiol. 86: 691-719, 1985.

32. Kirsch GE, Brown AM: Kinetic properties of single sodium channels in rat heart and rat brain. J. Gen. Physiol. 93: 85-99, 1989.

33. Trimmer JS, Cooperman SS, Tomiko SA, Zhou JY, Crean SM, Boyle MB, Kallen RG, Sheng ZH, Barchi RL, Sigworth FJ, Goodman RH, Agnew WS, Mandel G: Primary structure and functional expression of a mammalian skeletal muscle sodium channel. Neuron 3: 33-49, 1989.

34. Noda M, Shimizu S, Tanabe T, Takai T, Kayano T, Ikeda T, Takahashi H, Nakayama H, Kanaoka Y, Minamino N, Kangawa K, Matsuo H, Raftery MA, Hirose T, Inafama S, Hayashida H, Miyata T, Numa S: Primary structure of Electrophorus electricus sodium channel deduced from cDNA sequence. Nuture 312: 121-127, 1984.

35. Noda M, Ikeda T, Kayano T, Suzuki H, Takeshima H, Kurasaki M, Takahashi H, Numa S: Existence of distinct sodium channel messenger RNA in rat brain. Nature 320: 188-192, 1986.

36. Stuhmer W, Conti F, Suzuki H, Wang XD, Noda M, Yahagi N, Kubo H, Numa S: Structural parts involved in activation and inactivation of the sodium channel. Nature 339: 597-603, 1989.

37. Singh BN, Opie LH, Harrison DC, Marcus DI: Antiarrhythmic agents. In Opie LH., ed. Drugs for heart. Grune and Stratton Inc. Orlando, pp 54-90, 1987.

38. Harrison DC: Antiarrhythmic drug classification: new science and practical application. Am. J. Cardiol. 56: 185-187, 1985.

39. Nattel S: Antiarrhthymic drug classifications: A critical appraisal of their history, present status, and clinical relevance. Drugs. 41: 672-701, 1991.

40. Woosley RL: Antiarrhythmic drugs. Annu. Rev. Pharmacol. Toxicol. 31: 427-455, 1991.

41. Hondeghem LM, Katzung BG: Antiarrhythmic agents: The modulated receptor mechanism of action of sodium and calcium channel-blocking drugs. Ann. Rev. Pharmacol. Toxicol. 24: 387-423, 1984.

42. Courtney KR: Fast frequency-dependent block of action potential upstroke in rabbit atrium by small local anesthetics. Life Sci. 24: 1581-1588, 1979.

43. Colatsky TJ: Mechanisms of action of lidocaine and quinidine on action potential duration in rabbit cardiac Purkinje fibers: an effect on steady state sodium currents? Circ. Res. 50: 17-27, 1982.

44. Weld FM, Coromilas J, Rottman JN, Bigger JT: Mechanisms of quinidine induced depression of maximum upstroke velocity in ovine cardiac Purkinje fibers. Circ. Res. 50: 369-376, 1982.

45. Hondeghem LM, Katzung BG: Time and voltage-dependent interactions of antiarrhythmic drugs with cardiac sodium channels. Biochim. Biophys. Acta. 472: 373-398, 1977.

46. Hille B: Local anesthetics: Hydrophilic and hydrophobic pathways for the drug receptor reaction. J. Gen. Physiol. 69: 497-515, 1977.

47. Hondeghem L and Katzung BG: Test of a model of antiarrhythmic drug action-effects of quinidine and lidocaine on myocardial conduction. Circulation 61: 1217-1225, 1980.

48. Clarkson GW, Hondeghem LM: Evidence for a specific receptor site for lidocaine, quinidine and bupivacaine associated with cardiac sodium channels in guinea pig ventricular myocardium. Circ. Res. 56: 496-506, 1985.

49. Duff HJ, Roden DM, Primm RR, Oates JA, Woosley RL: Mexiletine in the treatment of resistant ventricular arrhythmias: enhancement of

efficacy and reduction of dose-related side effects by combination with quinidine. Circulation 67: 1124-1128, 1983.

50. Roden DM, Iansmith DH, Woosley RL: Frequency-dependent interaction of mexiletine and quinidine on depolarization and repolarization in canine Purkinje fibers. J. Pharmacol. exp. Ther. 243: 1218-1224, 1988.

51. Patt MV, Grossbard CL, Graboys TB, Lown B: Combination antiarrhythmic therapy for management of malignant ventricular arrhythmia. Am. J. Cardiol. 62: 181-211, 1988.

52. Starmer CF, Grant AO, Strauss HC: Mechanisms of use-dependent block of sodium channels in excitable membranes by local anesthetics. Biophys. J. 46: 15-27, 1984.

53. Sheldon RS, Cannon NJ and Duff HJ: A receptor for type I antiarrhythmic drugs associated with rat cardiac sodium channels. Cir. Res. 61: 492-497, 1987.

54. Sheldon RS, Cannon NJ, Nies AS, Duff HJ: Stereospecific interaction of tocainide with the cardiac sodium channel. Mol. Pharmacol. 33: 327-331, 1988.

55. Baumgarten CM, Makielski JC, Fozzard HA: External site for local anesthetic block of cardiac Na^+ channels. J. Mol. Cell. Cardial. 23 (suppl I): 85-93, 1991

56. Greenspan AM, Spielman SR, Webb CR, Sokoloff NM, Rae AP, Horowitz LN: Efficacy of combination therapy with mexiletine and a type 1A agent for inducible ventricular tachyarrhythmias secondary to coronary artery disease. Am. J. Cardiol. 56: 277-284, 1985.

57. Duff HJ, Mitchell LB, Manyari D, Wyse DG: Mexiletine-quinidine combination: electrophysiologic correlates of a favorable antiarrhythmic interaction in humans. J. Am. Coll. Cardiol 10: 1149-1156, 1987.

58. Giardina EGV, Wechsler ME: Low dose quinidine-mexiletine combination therapy versus quinidine monotherapy for treatment of ventricular arrhythmias. J. Am. Coll. Cardiol 15: 1138-1145, 1990.

59. Duff HJ, Kolodgie FD, Roden DM, Woosley RL: Electropharmacologic synergism with mexiletine and quinidine. J. Cardiovasc. Pharm. 8: 840-846, 1986.

60. Duff HJ, Gault NT: Mexiletine and quinidine in combination in an ischemic model: supra-additive antiarrhythmic and electrophysiological actions. J. Cardiovasc. Pharmacol. 8: 847-857, 1988.

61. Duff HJ: Mexiletine-quinidine combination: Enhanced antiarrhythmic and electrophysiologic activity in the dog. J. Pharmacol. exp. Ther. 249: 617-622, 1989.

62. Costand-Jaeckle A, Liem LB, Franz MK: Frequency-dependent of quinidine, mexiletine and their combination on postrepolarization refractoriness in vivo. J. Cardiovasc. Pharmacol. 14: 810-817, 1989.

63. Costand-Jaeckle A, Franz MK: Frequency-dependent antiarrhythmic drug effects on postrepolarization refractoriness and ventricular conduction time in canine ventricular myocardium in vivo. J. Pharmacol. exp. Ther. 251: 39-46, 1989.

64. Valois M, Sasyniuk BI: Modification of the frequency and voltage dependent effects of quinidine when administered in combination with tocainide in canine Purkinje fibers. Circulation 76: 427-441, 1987.

65. Valenzuela C, Sanchez-Chapula J: Electrophysiologic interactions between mexiletine-quinidine and mexiletine and ropitoin in guinea pig papillary muscle. J. Cardiovasc. Pharmacol. 14: 783-789, 1989.

66. Duff HJ, Cannon NJ, Sheldon RS: Mexiletine-quinidine in isolated hearts: an interaction involving the sodium channel. Cardiovasc. Res. 23: 584-592, 1989.

67. Duff HJ, Rahmberg M, Sheldon RS: Role of quinidine in the mexiletine-quinidine interaction: Electrophysiologic correlates of enhanced antiarrhythmic efficacy. J. Cardiovasc. Pharmacol. 16: 685-692, 1990.

68. Giles WR and Imaizumi Y: Comparison of potassium currents in rabbit atrial and ventricular cells. J. Physiol. 405: 123-145, 1988.

69. Kavanagh KM, Clark RB, Sanchez-Chapula JA, Salinas-Steffanon E, Rahmberg M, Lathrop D, Drury T, Giles WR, Duff HJ: Antiarrhythmic effects of barium-induced inhibition of an inwardly rectifying potassium current in the mammalian ventricle. Circ. Res. (submitted July, 1991)

70. Johns JA, Anno T, Bennett PB, Snyders DJ, Hondeghem LM: Temperature and voltage dependence of sodium channel blocking and

unblocking by O-demethyl-encainide in isolated guinea pig myocytes. J. Cardiovasc. Pharmacol. 13: 826-835, 1989.

71. Giles W, van Ginneken A, Shibata EF: Ionic currents underlying cardiac pacemaker activity: a summary of voltage-clamp data from single cells. In: Nathan RD., ed. Cardiac Muscle: the Regulation of Excitation and Contraction. Academic Press, Orlando, Fla. pp 1-27, 1986.

72. Makielski JC, Sheets MF, Hanck DA, January CT, Fozzard HA. Sodium current in voltage clamped internally perfused canine cardiac Purkinje cells. Biophys. J. 52: 1-11, 1987.

73. Clark RB, Giles WR: Sodium current in single cells from bull-frog atrium: Voltage dependence and ion transfer properties. J. Physiol. 391: 235-265, 1987.

74. Campbell TJ: Resting and rate-dependent depression of maximum rate of depolarization (Vmax) in guinea pig ventricular action potentials by mexiletine, disopyramide, and encainide. J. Cardiovasc. Pharmacol. 5: 291-296, 1983.

75. Campbell TJ: Kinetics of onset of rate-dependent effects of class I antiarrhythmic drugs are important in determining their effects on refractoriness in guinea-pig ventricle, and provide a theoretical basis for their subclassification. Cardiovasc. Res. 17: 344-352, 1983.

76. Hume JR and Uehara A: Ionic basis of the different action potential configurations of single guinea-pig atrial and ventricular myocytes. J. Physiol. 368: 525-544, 1985.

77. Mitchell MR, Powell T, Terrar DA, Twist VW: The effects of ryanodine, EGTA and low-sodium on action potentials in rat and guinea-pig ventricular myocytes: Evidence for two inward currents during the plateau. Br. J. Pharmacol. 81: 543-550, 1984.J.

78. Kiyosue T, Arita M: Late sodium current and its contribution to action potential configuration in guinea pig ventricular myocytes. Cir. Res. 64: 389-387, 1989.

79. Ono K, Kiyosue T, Arita M: Comparison of the inhibitory effects of lidocaine and mexiletine on the calcium current of single ventricular cells. Life Sci. 39: 1465-1470, 1986.

80. Stroobandt R, Kesteloot H: Effects of sotalol, aprindine and their combination on maximum upstroke velocity of action potential in guinea pig papillary muscle. Eur. J. Pharmacol. 131: 249-256, 1986.

81. Kohlhardt M, Seifert C: Properties of V_{max} block of I_{Na}-mediated action potentials during combined application of antiarrhythmic drugs in cardiac muscle. Naunyn-Schmiedebergs. Arch. Pharmacol. 330: 235-244, 1985.

82. Delpon E, Velenzuela C, Tamargo J: Electrophysiological effects of the combination of mexiletine and flecainide in guinea pig ventricular fibres. Br. J. Pharmacol. 103: 1411-1416, 1991.

83. Sunami A, Fan Z, Nitta JI, Hiraoka M: Two components of use-dependent block of Na^+ current by disopyramide and lidocaine in guinea pig ventricular myocytes. Circ. Res. 68: 653-661, 1991.

84. Brown AM, Lee KS, Powell T: Sodium current in single rat heart muscle cells. J. Physiol. 318: 479-500, 1981.

85. Weidmann S: The effect of the cardiac membrane potential on the rapid availability of the sodium carrying system. J. Physiol. 127: 213-224, 1955.

86. Cohen CJ, Bean BP, Tsien RW: Maximal upstroke velocity as an index of available sodium conductance: comparison of maximal upstroke velocity and voltage clamp measurements of sodium current in rabbit Purkinje fibers. Circ. Res. 54: 635-651, 1984.

87. Sheets MF, Hanck DA, Fozzard HA: Nonlinear relationship between V_{max} and I_{Na} in canine cardiac Purkinje cells. Circ. Res. 63: 386-398, 1988.

88. Allessie MA, Rensma PL, Brugada J, Smeets JLRM, Penn O, Kirchhof CJHJ: Pathophysiology of atrial fibrillation. In: Zipes DP and Jalife J eds., Cardiac Electrophysiology from Cell to Bedside. Philadelphia, W. B. Saunders, Co. pp 548-559, 1990.

89. Roberge FA, Drouhard JP: Using V_{max} to estimate changes in the sodium membrane conductance in cardiac cells. Comput. Biomed. Res. 20: 351-365, 1987.

90. Duker BG: Frequency dependent effects of tocainide, quinidine and flecainide on conduction as reflected in the rise time of the monophasic action potential in the isolated guinea pig heart. Cardiovas. Res. 25: 217-222, 1991.

91. Nattel S and Jing WH: Rate-dependent changes in intraventricular conduction produced by procainamide in anesthetized dogs. A quantitative analysis base on the relation between phase 0 inward current and conduction velocity. Circ. Res. 65: 1485-1498, 1989.

92. Buchanan JW Jr., Saito T and Gettes LS: The effects of antiarrhythmic drugs on stimulation frequency and potassium-induced resting membrane potential changes on conduction velocity and dv/dt (V_{max}) in guinea pig myocardium. Circ. Res. 56: 696-703, 1985.

93. Vanheel B, de-Hemptinne A, Leusen I: Intracellular pH and contraction of isolated rabbit and cat papillary muscle: effect of superfusate buffering.